

TERNARY PHASE EQUILIBRIA IN TRANSITION METAL-
BORON-CARBON-SILICON SYSTEMS

Part I. Related Binary Systems

Volume IX. Hf-B System

E. Rudy
St. Windisch

This document is subject to special export controls and each transmittal to foreign governments or foreign nationals may be made only with prior approval of Metals and Ceramics Division, Air Force Materials Laboratory, Wright-Patterson Air Force Base, Ohio.

*** Export controls have been removed ***

Approved for Public Release

FOREWORD

The work described in this report was carried out at the Materials Research Laboratory, Aerojet-General Corporation, Sacramento, California, under USAF Contract No. AF 33(615)-1249. The contract was initiated under Project No. 7350, Task No. 735001. The program is administered under the direction of the Air Force Materials Laboratory, Research and Technology Division, with Captain R. A. Peterson and Lt. P.J. Marchiando acting as Project Engineers and Dr. E. Rudy, Aerojet-General Corporation as Principal Investigator. Professor Dr. Hans Nowotny, University of Vienna, served as consultant to the project.

The project, which includes the experimental and theoretical investigation of related binary and ternary systems in the system classes Me -Me₂-C, Me-B-C, Me -Me₂-B, Me-Si-B, and Me-Si-C, was initiated on 1 January 1964.

The phase diagram work was performed by E. Rudy and St. Windisch. Assisting in the investigations were: J. Pomodoro (preparation of sample material), T. Eckert (DTA-runs), J. Hoffman (metallographic preparations), and R. Cobb (X-ray exposures).

Chemical analysis of the alloys was performed under the supervision of Mr. W. E. Trahan, Quality Control Division of Aerojet-General Corporation. The authors wish to thank Mr. R. Cristoni for the preparation of the illustrations and Mrs. J. Weidner, who typed the report.

The manuscript of this report was released by the authors October 1965 for publication as an RTD Technical Report.

Other reports issued under USAF Contract AF 33(615)-1249 have included:

Part I. Related Binaries

- Volume I, Mo-C System
- Volume II, Ti-C and Zr-C Systems
- Volume III, Systems Mo-B and W-B
- Volume IV, Hf-C System
- Volume V, Ta-C System. Partial Investigations in the systems V-C and Nb-C
- Volume VI, W-C System. Supplemental Information on the Mo-C System
- Volume VII, Ti-B System
- Volume VIII, Zr-B System

Part II. Ternary Systems

- Volume I, Ta-Hf-C System
- Volume II, Ti-Ta-C System
- Volume III, Zr-Ta-C System
- Volume IV, Ti-Zr-C, Ti-Hf-C, and Zr-Hf-C Systems

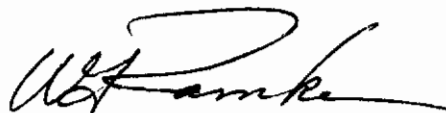
Contrails

FOREWORD (Cont'd)

Part III. Special Experimental Techniques
Volume I, High Temperature Differential Thermal
Analysis

Part IV. Thermochemical Calculations
Volume I, Thermodynamic Properties of Group IV,
V, and VI Transition Metal Carbides

This technical report has been reviewed and is approved.



W. G. RAMKE
Chief, Ceramics and Graphite Branch
Metals and Ceramics Division
Air Force Materials Laboratory

ABSTRACT

The binary alloy system hafnium-boron has been investigated by means of X-ray, metallographic, melting point, and differential-thermo-analytical techniques. The experimental alloy material comprised of hot-pressed and heat-treated, arc- and electron-beam melted, as well as equilibrated and quenched alloy material. All phases of the experimental investigations were supported by chemical analysis.

The results of the present investigation, which resulted in the establishment of a complete phase diagram for the system, are discussed and compared with previously established system data.

TABLE OF CONTENTS

	PAGE
I. INTRODUCTION AND SUMMARY	1
A. Introduction	1
B. Summary	1
II. LITERATURE REVIEW.	4
III. EXPERIMENTAL PROGRAM	6
A. Starting Materials	6
B. Experimental Procedures	8
1. Sample Preparation and Heat Treatment.	8
2. Differential Thermal Analysis	9
3. Determination of Melting Points	9
4. X-ray Investigations	10
5. Chemical Analysis	10
6. Metallographic Procedures	11
C. Results	11
1. The Hafnium Phase	11
2. The Concentration Range Hafnium-Hafnium Diboride	18
3. Hafnium Diboride, and Boron-Rich Equilibria.	32
IV. DISCUSSION	41
References	42

ILLUSTRATIONS

FIGURE		PAGE
1	Constitution Diagram Hafnium-Boron	3
2	Melting Temperatures and Solid State Reaction Isotherms in the Hafnium-Boron System	14
3	Hf-B (1 At% B), Quenched from 2000°C	15
4	Hf-B (1.8 At% B), Quenched from 2120°C	15
5	Hf-B (4 At% B), Quenched from 2000°C	16
6	α - β -Transformation in Boron-Desoxidized Hafnium (A) and in a Hafnium - 6 Atomic Percent Boron Alloy.	17
7	DTA-Thermogram (Cooling) of a Hafnium-Boron Alloy with 6 Atomic Percent Boron	18
8	Hf-B (10 At% B), Rapidly Quenched from 1900°C	19
9	Hf-B (13 At% B), Rapidly Quenched from 1900°C	20
10	Hf-B (20 At% B), Quenched with 8°C per Second from 1900°C	20
11	Hf-B (30 At% B), Quenched with Approximately 20°C per Second from 1910°C	21
12	DTA-Thermogram of a Hafnium-Boron Alloy with 40 Atomic Percent Boron	22
13	DTA-Thermograms (Cooling) of Hafnium-Boron Alloys from the Concentration Range 50 to 60 At% B	23
14	Hf-B (30 At% B), Cooled with 3°C per Second from 2130°C	24
15	Hf-B (35 At% B), Cooled with 8°C per Second from 2150°C	24
16	Hf-B (30 At% B), Alloy from Figure 14, Annealed for 225 hrs at 1650°C	25
17	Hf-B (40 At% B), Reannealed for 225 hrs at 1650°C after Rapid Quenching from 2500°C	26
18	Hf-B (40 At% B), Quenched from 2500°C	26
19	Hf-B (40 At% B), Quenched from 2500°C. Annealing: 2 Minutes at ~1950°C, Followed by 225 hrs at 1650°C	27
20 a) and b)	Hf-B (46 At% B), Quenched from 2600°C	28

ILLUSTRATIONS (Cont.)

FIGURE		PAGE
21	Hf-B (46 At% B), Quenched from 2500°C	29
22 a) through 22d)	Hf-B (48 At% B), Quenched from 2600°C	29
23	Lattice Parameters of Hafnium Diboride as a Function of the Boron Concentration.	33
24	Hf-B (63.0 At% B), Rapidly Cooled from 2600°C	34
25	Hf-B (64.8 At% B), Rapidly Cooled from 2600°C	34
26 a) through 26 i)	Microstructures of High-Temperature Quenched Hafnium-Boron Alloys from the Concentration Range 65 to 72 Atomic Percent	35
27	DTA-Thermogram of a Hafnium-Boron Alloy with 80 Atomic Percent Boron.	40

TABLES

TABLE		PAGE
1	Isothermal Reaction in the System Hafnium-Boron	4
2	Structure and Lattice Parameters of Hafnium-Boron	6
3	Melting Temperatures of Hafnium-Boron Alloys and Qualitative Phase Evaluation	12

I. INTRODUCTION AND SUMMARY

A. INTRODUCTION

In spite of the increased interest in hafnium-boron alloys over the past few years — hafnium diboride is the most oxidation resistant boride known to date⁽¹⁾ — comparatively little is known about the high temperature phase relationships in this system. Data of interest concern the melting temperature of the diboride phase and its range of homogeneity as a function of temperature; further, in view of the possibility of using diborides as container material for boron melts, temperature and composition of the boron-rich eutectic; and finally, the equilibria on the metal-rich side of the system are of importance in connection with the binder problem for the extreme brittle borides.

In view of the scarcity of data available for this alloy system, a fairly thorough investigation of the entire phase diagram was undertaken. Difficulties encountered during the course of the work are inherent to the whole system class, and included slow attainment of equilibrium in solid-state equilibration studies, severe melting point depressions for the extreme high melting diboride phase upon small contaminant concentrations, and the general problem of obtaining dense and homogeneous alloy material required for good metallographic work.

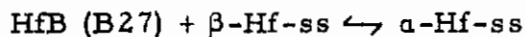
B. SUMMARY (Figure 1 and Table 1)

Two intermediate phases, a peritectically decomposing, orthorhombic monoboride of low stability, and a very refractory diboride of hexagonal structure, are formed in this alloy system. The previously reported face-centered cubic monoborides does not exist.

1. The Hafnium Phase

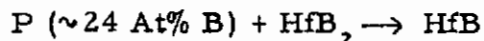
β -hafnium melts at $2218 \pm 6^\circ\text{C}$. The low temperature, hexagonal close-packed (α) modification, transforms at $1795 \pm 35^\circ\text{C}$ (extrapolated to 100% Hf) into the body-centered cubic high temperature (β) allotrope.

β -Hf enters a eutectic reaction with the monoboride; the eutectic point is located at $13 \pm 2 \text{ At\% B}$ and a temperature of $1880 \pm 15^\circ\text{C}$. The solid solubility of boron in β -Hf at this temperature is less than 2 atomic percent, and boron additions have little effect upon the α - β -transformation in hafnium. Nevertheless, a slight increase (1795° for pure hafnium, to $1800 - 1820^\circ\text{C}$ in excess monoboride containing alloys) is observed, which suggests a peritectoid reaction process in the binary:



2. Hafnium Monoboride (B27)

Hafnium monoboride probably occurring with a boron defect of approximately one (1) atomic percent, has an orthorhombic B27 (FeB)-type of crystal structure ($a = 6.51_7 \text{ \AA}$; $b = 3.21_8 \text{ \AA}$; $c = 4.92_0 \text{ \AA}$). The phase, which has a negligible range of homogeneity, forms in a peritectic reaction at 2100°C from diboride and melt according to:



The phase forms by nucleation in hafnium or the hafnium-rich melt. The nucleation reaction appears to be very slow at temperatures below $\sim 1650^\circ\text{C}$; thus, the monoboride cannot be obtained within feasible lengths of time upon reannealing of high-temperature ($>2200^\circ\text{C}$)-quenched alloys at lower temperatures. Although not specifically investigated and therefore unproven, there are indications, that the monoboride is unstable below $\sim 1250^\circ\text{C}$, decomposing in an extremely slow reaction into α -hafnium and the diboride.

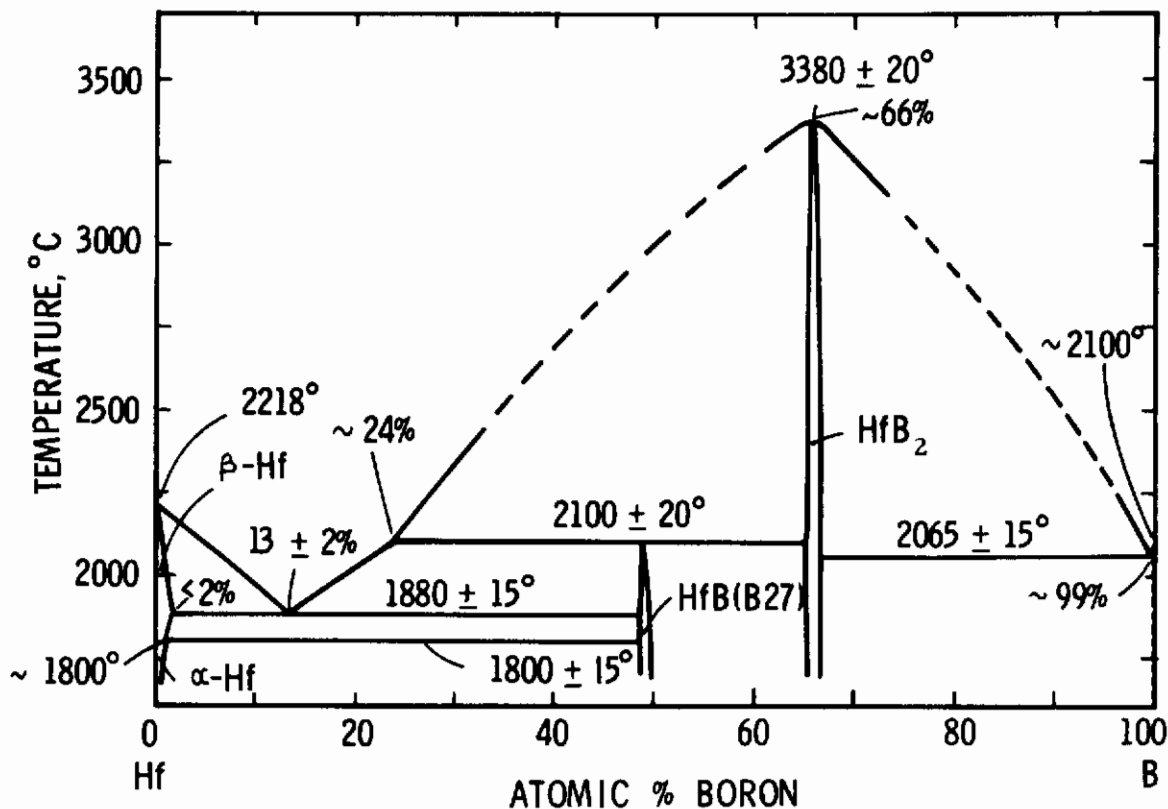


Figure 1. Constitution Diagram Hafnium-Boron.

3. Hafnium Diboride

Hafnium diboride, with an hexagonal, C32 (AlB₂)-type of crystal structure ($a = 3.142 \text{ \AA}$; $c = 3.447 \text{ \AA}$) and a negligible range of homogeneity (<2 At% B) over its entire temperature range of existence, melts congruently at 3380°C at the stoichiometric composition. The phase enters a eutectic equilibrium (~ 99 At% B, 2065°C) with boron.

Table 1. Isothermal Reactions in the System Hafnium-Boron

Temperature, °C	Reaction	Compositions of the Equilibrium Phases, At%B			Type of Reaction
3380°	$L \rightarrow \text{HfB}_2$	66	66	--	Congruent Transformation
2218°	$L \rightarrow \beta\text{-Hf}$	0	0	--	Melting Point of Hafnium
2100°	$L + \text{HfB}_2 \rightarrow \text{HfB}$	24	65	49	Peritectic Reaction
2100°	$L \rightarrow \text{B}$	100	100	--	Melting Point of Boron
2065°	$L \rightarrow \text{HfB}_2 + \text{B}$	~99	66.6	100	Eutectic Reaction
1880°	$L \rightarrow \beta\text{-Hf} + \text{HfB}$	13	<2	~49	Eutectic Reaction
~1800°	$\beta\text{-Hf} + \text{HfB} \rightarrow \alpha\text{-Hf}$	~1	~49	<1	Peritectic Reaction
1795°	$\beta\text{-Hf} \rightarrow \alpha\text{-Hf}$	0	0	--	α - β -Transformation in Hafnium
<1250°	$\text{HfB} \rightarrow \alpha\text{-Hf} + \text{HfB}_2$	~49	<1	~66	Eutectoid Decomposition of HfB*

* Not fully ascertained

II. LITERATURE REVIEW

Two intermetallic phases, a refractory diboride with a hexagonal structure, and a monoboride with an orthorhombic (B27) structure are formed in this alloy system. The previously reported face-centered cubic (B1) monoboride does not exist.

Hafnium diboride, isomorphous with the other diborides of the group IV, V, and VI metal diborides, has a hexagonal, C32 (AlB_2)-type of crystal structure with $a = 3.141 \text{ \AA}$, and $c = 3.470 \text{ \AA}$ (2). Melting temperatures

Contrails

reported for this phase include: $\sim 3100^{\circ}\text{C}$ (K. Moers, 1931⁽³⁾); C. Agte and K Moers, 1931⁽⁴⁾, 3240°C (F. W. Glaser, et.al. 1953⁽²⁾), and 3060°C (R. Kieffer, et.al., 1952⁽⁵⁾).

In addition to the diboride, a face-centered cubic (B1) compound with a lattice parameter of $a = 4.62 \text{ \AA}$ was observed by P. W. Glaser, et.al. ⁽²⁾ in hot-pressed hafnium-boron alloys, and attributed to a phase HfB. Later investigations by E. Rudy and F. Benesovsky⁽⁶⁾ on high purity sample material showed that the true binary compound is orthorhombic (B27-type), with $a = 6.517 \text{ \AA}$; $b = 3.218 \text{ \AA}$, and $c = 4.919 \text{ \AA}$, and that the previously observed B1-phase probably corresponded to an impurity phase Hf (O, N, C). This latter interpretation is also suggested by a comparison of the lattice parameters, since the cell dimension given for the 'monoboride' generally lie between those of the binary compounds of hafnium with the corresponding impurity elements: $a_{\text{HfC}_{1-x}} = 4.61 \text{ to } 4.64 \text{ \AA}$; $a_{\text{HfN}_{1-x}} = 4.525 \text{ to } 4.52 \text{ \AA}$. A cubic (B1) monoboride would have the much larger parameter of $\sim 4.70 \text{ \AA}$ ⁽⁶⁾.

Structural details on hafnium borides as well as a collection of lattice parameter data are presented in Table (2).

No systematic phase diagram investigations were carried out in the system, and tentative diagrams proposed^(7, 8) were mainly based on estimates. Recently, L. Kaufman and E. V. Clougherty⁽¹⁾ have measured a eutectic temperature (Hf + HfB) of 1960°C , and a peritectic decomposition temperature for HfB in excess of 2400°C .

For detailed reference on earlier work and a summary of the physical properties of hafnium borides, R. Kieffer and F. Benesovsky's book "Hartstoffe"⁽⁹⁾ may be consulted.

Table 2. Structure and Lattice Parameters of Hafnium Borides

Phase	Structure	Lattice Parameters, Å	
		Literature Values	This Investigation
HfB*	Cubic, B1	4.62 (2)	not confirmed
HfB	Orthorhombic B27-type(FeB)	a = 6.517 Å b = 3.218 Å (6, 7) c = 4.919 Å	a = 6.517 Å b = 3.218 Å c = 4.920 Å
HfB ₂	Hexag. C32-type (AlB ₂)	a = 3.141 c = 3.470 (2)	a = 3.142 Å c = 3.477 Å (Hf _{0.96} Zr _{0.04} B ₂)

*Probably Impurity Phase Hf (N, O, B, C).

III. EXPERIMENTAL PROGRAM

A. STARTING MATERIALS

The elements as well as hafnium diboride served as the starting materials for the experimental investigations.

Hafnium sponge and hafnium metal powder (<120 μ) were purchased from Wah Chang Corporation, Albany, Oregon. Their analyses were as follows: Hafnium metal (contents in ppm); Al-20, C-210, Nb-680 (<1000)*, Cr-<20, Cu-40, Fe-265, H-55, Mo-40, N-200 (<300), O-810 (<1000), Si-<40 (10), Ta-<200 (400), Ti-20, W-235, sum of all other impurities-<100. The hafnium powder, which also contained 4.1 atomic percent zirconium, had lattice parameters of a = 3.19₆ Å; c = 5.05₇ Å, which compare favorably with reported literature values of a = 3.194 to 3.199 Å, and c = 5.0510 to 5.062 Å⁽¹⁰⁾.

*The concentration figures given in the brackets are data from a control analysis performed at the Analytical Chemistry Laboratory at Aerojet-General Corporation.

Contrails

The hafnium sponge had the following impurities (contents in ppm): Al-94, Cu-<40, Fe-185, Cl-100, Mg-450, N-30, O-680, Si-<40, Ti-250, W-<7. The zirconium content of the sponge was 4 atomic percent. The DTA - analyses, which yielded apparent transformation temperatures of 1770 to 1800°C for the arc molten metal powder and the sponge hafnium, are compatible with the values to be expected from the combined interstitial impurity contents⁽¹¹⁾.

Boron powder in a purity of 99.55% was purchased from United Mineral and Chemical Corporation, New York. Major impurities were iron (0.25%) and carbon (0.1%).

The diboride powder was prepared by direct combination of the elements at high temperatures. Hafnium and boron react violently to form the diboride; therefore, a master alloy containing 85 atomic percent boron was prepared first, which then was reacted in second step with the necessary amount of hafnium to form the stoichiometric diboride. The detailed procedures followed were analogous to those described for zirconium diboride in a previous report⁽¹²⁾. After the final reaction, which was allowed to proceed at temperatures between 1800 and 2000°C, the reaction lumps were crushed and comminuted by ball-milling to a grain size smaller than 47 micrometers. Cobalt and other metallic impurity traces, which were picked up during milling, were removed by an acid-leach in hot, 8 normal mixture of hydrochloric and sulfuric acid.

The chemical analysis of the diboride powder, which contained metallographically detectable quantities of monoboride, gave an average boron content of 65.0 ± 0.3 atomic percent; it also contained 0.018 Wt% carbon. Oxygen, nitrogen, and hydrogen were present in quantities less than 200 ppm.

A semiquantitative spectrographic analysis indicated the following additional impurities (in ppm): Fe-<200, Si-<200, Mg-<100, Ca-<500, Co, Ni, Mn, Cr, Mo-<100, Ti-300. V, W, Ta, and Nb were below the detectable level.

B. EXPERIMENTAL PROCEDURES

1. Sample Preparation and Heat Treatment

A total of 85 alloys were prepared for melting point, DTA, metallographic, and X-ray studies on solid state equilibrated samples.

Specimens with boron concentrations in excess of 60 atomic percent were hot-pressed, while for the preparation of metal-richer compositions the cold pressing-sintering route was chosen. The elemental powders were used as starting materials for the latter alloys, since equilibrium in sintered mixtures of hafnium and hafnium diboride could not be attained within feasible lengths of time. In addition to the hot- and cold-pressing, a number of specimens were arc- or electron-beam melted prior to the measurements or the homogenization treatments.

The samples which were loaded in a tantalum container, were homogenized in a tungsten-mesh element furnace manufactured by the R. Brew Company. Main equilibration temperature for the study of the solid state portion of the system was 1400°C (80 hrs); additional homogenization treatments were carried out at 1250°C (140 hrs), 1600°C (60 hrs), 1800°C (10 hrs), and 2000°C (2 hrs), and the formation of the monoboride in high-temperature quenched specimens was studied in a series of long-time heat-treatments (60 to 440 hrs) at temperatures varying between 1450 and 1800°C. Rapid quenching of the alloys after equilibration at temperatures in excess of 2000°C was achieved by dropping the resistively heated specimens into a tin bath, which was preheated to 300°C.

Contrails

Approximately one-fourth of the experimental alloys, the majority of which were located at compositions close to the mono- and the diboride, were chemically analyzed after the runs. With the exception of electron-beam and arc melted specimens, which showed composition shifts up to 3 atomic percent, the concentration stability of the samples was usually better than one atomic percent with regard to the weighed-in compositions.

2. Differential Thermal Analysis

Details of the DTA-setup and the calibration procedures have been described earlier^(13, 15). Specimens with boron concentration below 50 atomic percent were run under vacuum as well as under a protective atmosphere of 1/2 atm high purity helium: the furnace chamber was pressurized with high purity helium to approximately 1 1/2 atmospheres for higher-boron alloys. To retard interaction between the test samples and the container in the DTA-experiments, the walls of the graphite sample holder were lined with either tantalum or hafnium diboride; this particular choice of liner materials limited the useful operating range to temperatures below 2450°C.

3. Determination of Melting Points

The melting temperatures of the alloys were determined using the previously described⁽¹³⁾ Pirani-technique: A small sample bar, with dimensions varying between 4 x 4 x 20 mm to 10 x 10 x 40 mm in length, is clamped between two water-cooled copper-electrodes, and heated resistively to the temperature of the phase change. The temperatures are measured optically with a disappearing-filament type pyrometer through a quartz window in the furnace wall. A small black body hole, generally in the

Contrails

order of 0.6 mm in diameter and 3-4 mm in depth, drilled or pressed into the sample, serves as the reference point for the measurements.

Since this technique essentially eliminates the container problem, and the large transmission of 0.92 of the system implies only small temperature corrections, consistencies of $\pm 10^\circ\text{C}$ at 3000°C in homogeneously melting alloys are common. The overall temperature uncertainties are composed of two parts: The precision (consistency) of the measurements, and the uncertainties in the pyrometer calibration. They can be computed from the relation $\bar{\sigma} = \pm \sqrt{\sigma_c^2 + \sigma_m^2}$, where $\bar{\sigma}$ stands for the overall temperature uncertainty, and σ_c and σ_m designate standard error of the pyrometer calibration and precision of individual measurements, respectively. Typical calibration uncertainties are $\pm 10^\circ\text{C}$ at 2300°C , $\pm \sim 17^\circ\text{C}$ at 3000°C , and 30°C (estimated) at 4000°C . These values, in conjunction with the precision of the measurements referred to on the figures and in the text, may be used to calculate the overall temperature uncertainties involved in our measurements.

4. X-Ray Investigations

Since the structure of all phases occurring in this alloy system were known from previous work, only powder diffraction patterns with Cu-K_α -radiation were prepared from the alloys. The exposures were made in a 57.4 mm camera on a Siemens Crystalloflex II unit, and a Siemens-Kirem coincidence scale with micrometer attachment was used for measuring the films.

5. Chemical Analysis

The principle of the wet-chemical method used for the boron analysis consists in converting bound or free boron to boric acid, which then — after removal of interfering accompanying elements — is

Contrails

determined by differential titration of the complex acid formed with mannitol. The detailed procedures were analogous to those employed for titanium-boron alloys and have been described in an earlier report⁽¹⁴⁾.

The standard combustion technique in conjunction with a conductometric analysis for CO_2 was used for the determination of the total carbon content. Oxygen and nitrogen were hot-extracted in a gas-fusion apparatus using a platinum bath, and small impurity contents were determined in a semiquantitative way spectrographically.

6. Metallographic Procedures

The specimens were mounted in a combination of diallyl-phtalate and lucite-coated copper powder such as to provide an electrically conductive path from the top of the mount to the polished sample surface. After coarse grinding on silicon carbide paper with grit sizes between 120 to 600, the samples were mechano-chemically polished, using a slurry of 0.3 micrometer alumina and Murakami's solution on a nylon cloth. Excellent contrasts between the various phases in the system could be obtained by electro-etching in 2% NaOH: The hafnium phase was stained light-blue and HfB appeared light-brown in color, while the diboride essentially remained unaffected by the anodizing treatment. No etching was required for excess boron-containing alloys.

C. RESULTS

1. The Hafnium Phase

For hafnium, a melting point of $2218 \pm 6^\circ\text{C}$ was derived from four measurements on cold-pressed and sintered samples, as well as from DTA-measurements. Melting in the alloys with 2 and 5 atomic percent is already two-phased and occurs at significantly lower temperatures

Table 3: Melting Temperatures of Hafnium-Boron Alloys and Qualitative Phase Evaluation.

No. Nom. Anal.	Melting Temps. °C		Melting	X-Ray		Metallography		
	Incipient	Collapse		Phases	Lattice Parameters, Å			
1	0	n.d.	2218+6	2218+6 ↓	Sharp	n.d.	Single Phase Hf	
2	2	1.8	2041	2122 ↓	heterog	Hf + HfB	Hf: a=320 Å; c=5.07 Å	
3	5	4.9	1904	1973 ↓	heterog	Hf + HfB	n.d.	
4	10	10	1872	1905 ↓	sl. heterog	Hf + HfB	n.d.	Hf + (Hf + HfB) Eutec.
5	15	n.d.	1878	1878 ↓	sharp	n.d.	n.d.	HfB + (Hf + HfB) Eutec.
6	20	n.d.	1885	1897 ↓	heterog	n.d.	Hf: a=3.20 Å; c=5.08 Å	HfB + (Hf + HfB) Eutec.
7	23	n.d.	1896	1905 ↓	heterog	n.d.	n.d.	n.d.
8	25	n.d.	1898	1908 ↓	heterog	Hf + HfB	n.d.	n.d.
9	28	n.d.	1894	1903 ↓	heterog	Hf + HfB	n.d.	n.d.
10	30	n.d.	1882	1911 ↓	heterog	Hf + HfB + Trace HfB ₂	n.d.	n.d.
11	35	n.d.	1900	2022 ↓	heterog	Hf + HfB	HfB: a=6.518 Å; b=3.21 Å; c=4.92 Å	HfB + Hf
12	37	n.d.	1903	2024 ↓	heterog	Hf + HfB	n.d.	HfB + Hf + Trace HfB ₂
13	40	n.d.	1899	2044 ↓	heterog	Hf + HfB	HfB: a=6.51 Å; b=3.21 Å; c=4.91 Å	HfB + Hf
14	45	n.d.	1906	2033 ↓	heterog	Hf + HfB	HfB: a=6.51 Å; b=3.21 Å; c=4.92 Å	HfB + Hf
15	48	47	1995	2111 ↓	heterog	Hf + HfB + HfB ₂	n.d.	Hf + HfB + HfB ₂
16	50	48.5	2065	2158 ↓	heterog	Hf + HfB + HfB ₂	n.d.	Hf + HfB ₂ + Little HfB
17	51	50.5	2102	2189 ↓	heterog	Hf + HfB + HfB ₂	HfB: a=6.51 Å; b=3.21 Å; c=4.92 Å	Hf + HfB ₂ + Trace HfB
18	53	n.d.	2120	2343 ↓	heterog	Hf + HfB ₂	n.d.	Hf + HfB ₂ + Trace HfB
19	57	n.d.	2148	2456 ↓	heterog	Hf + HfB ₂ + Trace HfB	n.d.	Hf + HfB ₂
20	60	60	2212	2620 ↓	heterog	Hf + HfB ₂	n.d.	Hf + HfB ₂
21	62	62	2199	3012 ↓	heterog	HfB ₂	HfB ₂ : a=3.477 Å; c=3.142 Å	Hf + HfB ₂
22	63	n.d.	2756	3182 ↓	heterog	HfB ₂	HfB ₂ : a=3.477 Å; c=3.14 Å	Hf + HfB ₂
23	64	63.0	3205+25	3317+28	heterog	HfB ₂	n.d.	HfB ₂ + Little Hf
24	65	n.d.	3334+30	3346+18	fairly sharp	HfB ₂	HfB ₂ : a=3.474 Å; c=3.14 Å	HfB ₂ + Trace Hf

Table 3 (continued)

No. Nom. Anal.	Melting Temps. °C		Melting	X-Ray		Metallography
	Incipient	Collapse		Phases	Lattice Parameters, Å	
25 66 65.7	3380+20	3380+20	sharp	HfB ₂	HfB ₂ ; a=3.476Å; c=3.142Å	HfB ₂
26 67 66.4	3346+25	3346+25	fairly sharp	HfB ₂	HfB ₂ ; a=3.476Å; c=3.142Å	HfB ₂ + Trace B
27 68 67.4 2	2446	3255	heterog	HfB ₂	HfB ₂ ; a=3.477Å; c=3.142Å	HfB ₂ + B
28 69 68.6	2200	3140	heterog	HfB ₂	n. d.	HfB ₂ + B
29 72 71	2058	3098	heterog	HfB ₂	HfB ₂ ; a=3.477Å; c=3.142Å	HfB ₂ + B
30 75 n. d.	2065	2598	heterog	HfB ₂	n. d.	HfB ₂ + B
31 90 n. d.	2080	2140	heterog	HfB ₂ + B	n. d.	HfB ₂ + B

Legend: ↓ quenched
n. d. not determined

(Table 3 and Figure 2). Metallographically, an alloy with 1 atomic percent boron, quenched from 2000°C is single phase at high temperatures (Figure 3). The sample with ~2 atomic percent boron, prepared under similar conditions, already shows scant traces of excess monoboride (Figure 4), which becomes clearly recognizable in the alloy with a boron content of 4 atomic percent (Figure 5).

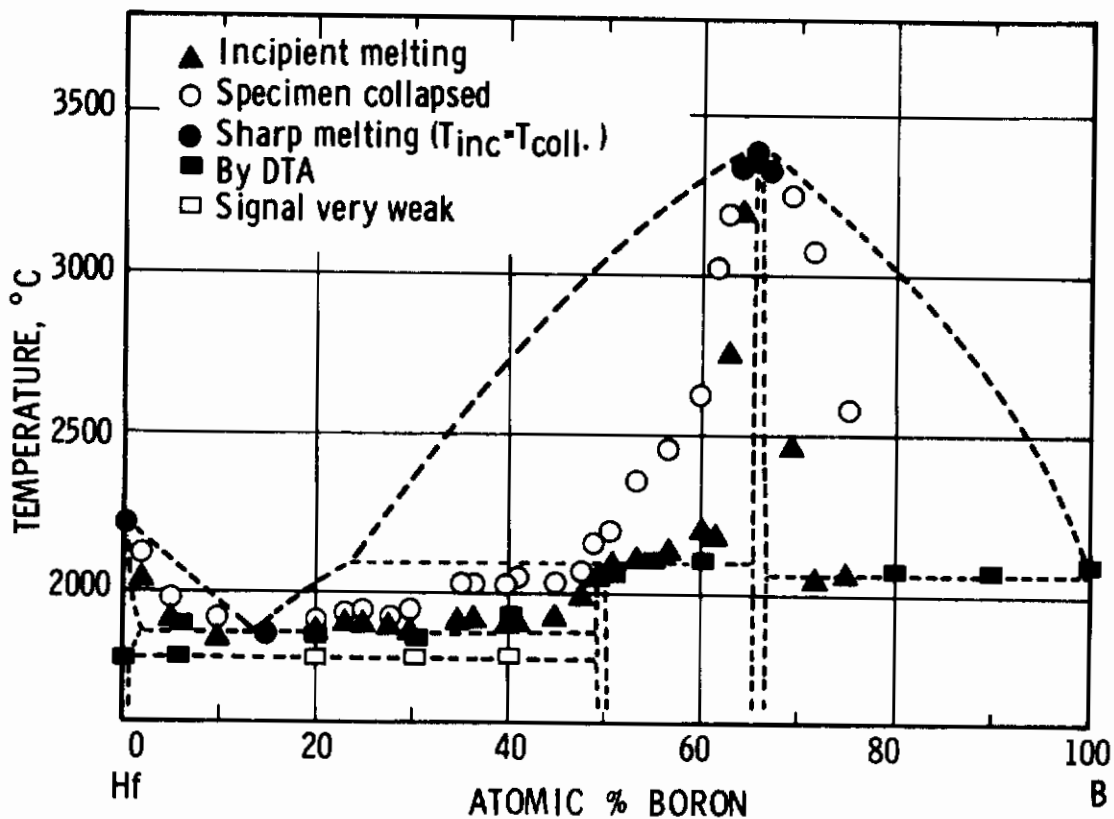


Figure 2. Melting Temperatures and Solid State Reaction Isotherms in the Hafnium-Boron System.

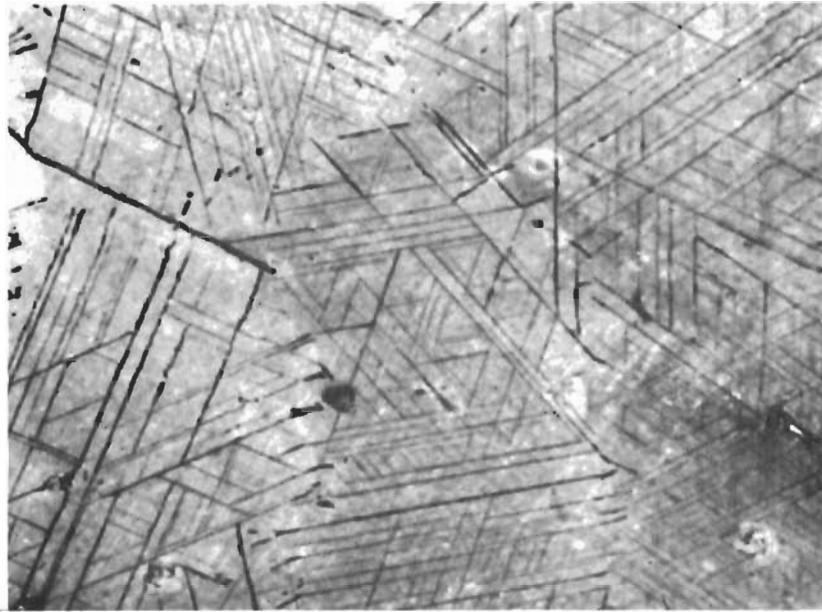


Figure 3. Hf-B (1 At% B), Quenched from 2000°C.

X1000

β -Hafnium (Transformed) and Small Amounts of Monoboride Precipitations.

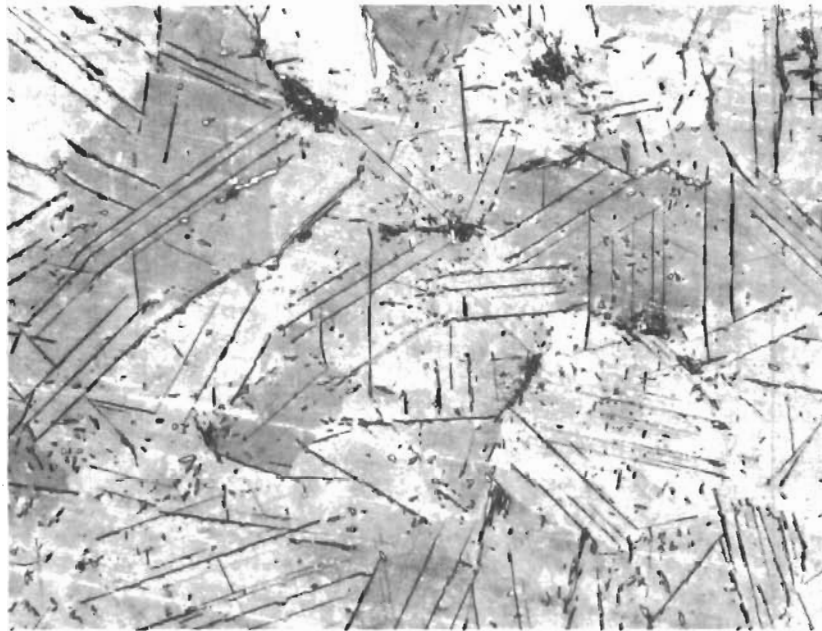


Figure 4. Hf-B (1.8 At% B), Quenched from 2120°C.

X550

β -Hafnium (Transformed) with Monoboride Precipitations and Traces of Excess Monoboride.

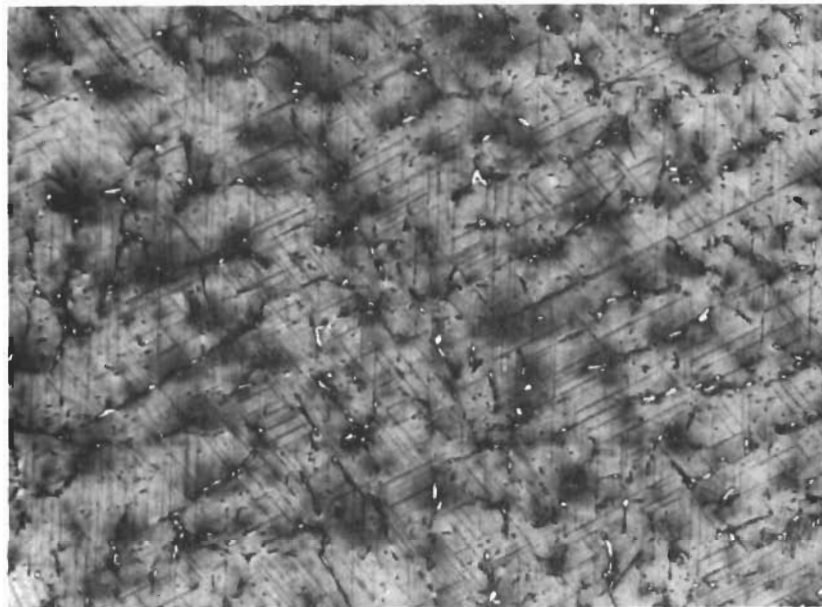


Figure 5. Hf-B (4 At% B), Cooled with 4°C per Second X250
from 2000°C.
β-Hafnium (Transformed), and Excess Monoboride.

Addition of 1 atomic percent to boron prior to electron-beam melting resulted in a lowering of the apparent transformation temperatures from $\sim 1800^{\circ}\text{C}$ for the hafnium starting material (Section III-A), to $\sim 1770^{\circ}\text{C}$ in the low-boron alloy. On the other hand, the thermal arrest due to the α - β -transformation reaction appeared consistently at about 1800°C in two-phased alloys Hf + HfB (Figure 6). A correlation of the data with post-melting chemical analysis, however, revealed, that in the 1 atomic percent alloy practically all the boron had combined with the oxygen impurities present in the starting material to form B_2O_3 , which then volatilized during the melting process; thus, one may assume, that the transformation temperatures measured in this alloy (Curve A in Figure 6) probably correspond close to that of pure hafnium, whereas the thermal arrests observed in the higher-boron-alloys are representative of the temperature for the corresponding reaction

Contrails

isotherm in the binary system. The apparent increase of the transformation temperature thus suggests the formation of the α -modification in a peritectoid reaction according to:

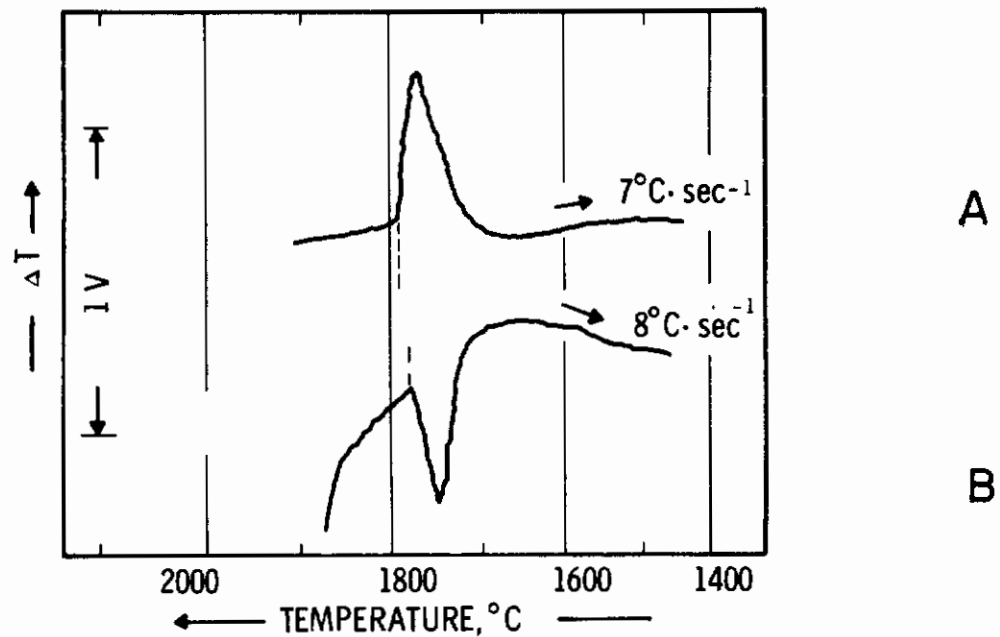


Figure 6. α - β -Transformation in Boron-Desoxidized Hafnium (A) and in a Hafnium - 6 Atomic Percent Boron Alloy (B). (Electron-Beam Molten Alloys; Zr-Content After Melting: ~ 1.9 At%).

i.e., the hexagonal close-packed α -modification is stabilized to slightly higher temperatures by dissolving small amounts (≤ 1 At%) of boron. A small, but finite boron solubility is also indicated by the slight increase of the lattice parameters of the metal-phase upon addition of boron: In the average, parameters of $a = 3.20 \text{ \AA}$, and $c = 5.07 \text{ \AA}$ were obtained for the metal phase in excess monoboride containing alloys, which are noticeable larger than the

lattice dimensions of the starting material, for which $a = 3.19_6 \text{ \AA}$ and $a = 5.05_7 \text{ \AA}$ were measured.

2. The Concentration Range Hafnium-Hafnium Diboride

While melting of the samples with boron concentrations of 5 and 10 atomic percent respectively was still two-phased, the alloy with 15 atomic percent boron melted isothermal (Table 3). Two-phase melting was again noticed in the specimens with boron contents above 20 atomic percent.

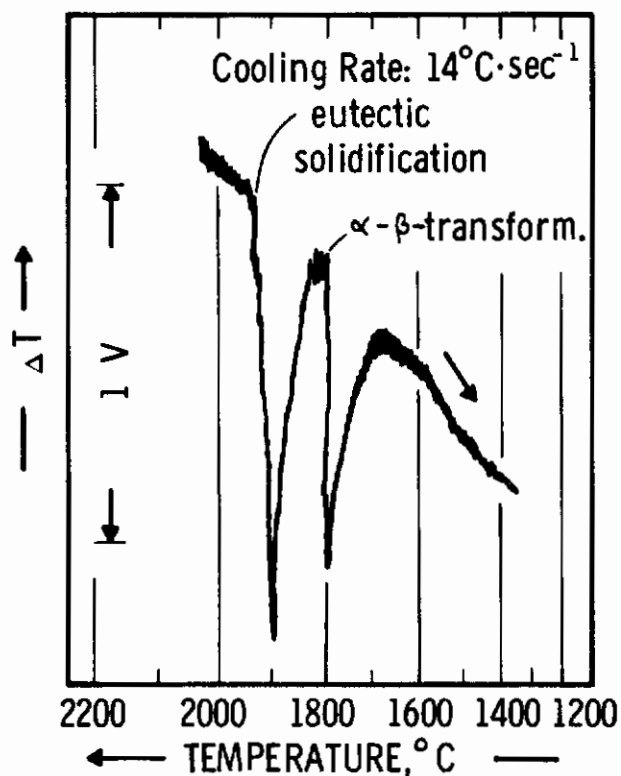


Figure 7. DTA-Thermogram (Cooling) of a Hafnium-Boron Alloy with 6 Atomic Percent Boron.

From the melting point measurements as well as the differential-thermoanalytical studies (Figure 7) a temperature of $1880 \pm 15^\circ\text{C}$ was derived for the metal-rich eutectic reaction isotherm, and the composition of the eutectic was bracketed to $13 \pm 2 \text{ At\% B}$ by metallographic inspection

Contrails

of specimens quenched from temperatures above the eutectic line (Figures 8 and 9). Similar as experienced during the investigation of the titanium- and zirconium-boron systems, the boride phases tend to segregate very rapidly to the metal-grain boundaries (Figure 10 and 11), and rapid quenching ($>300^{\circ}\text{C}$ per second) proved to be a necessity for retaining the eutectic structure.

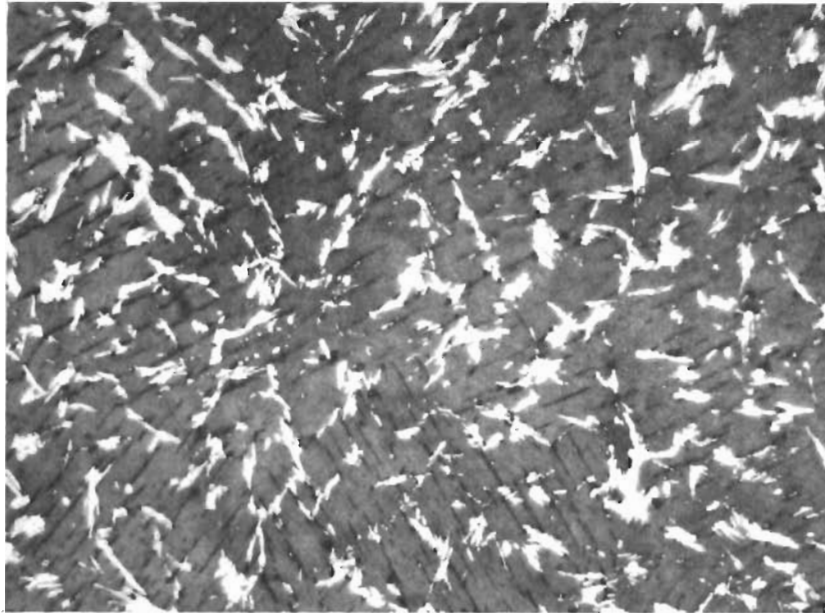


Figure 8. Hf-B (10 At% B), Quenched from 1900°C .

X500

Primary β -Hafnium (Transformed), and Hf + HfB Eutectic.

As the equi-atomic concentration region is approached, the incipient melting temperatures for the alloys increase to approximately 2100°C , but melting always remains two-phased, indicating a peritectic reaction isotherm at this temperature (Figure 2). The first appearance of

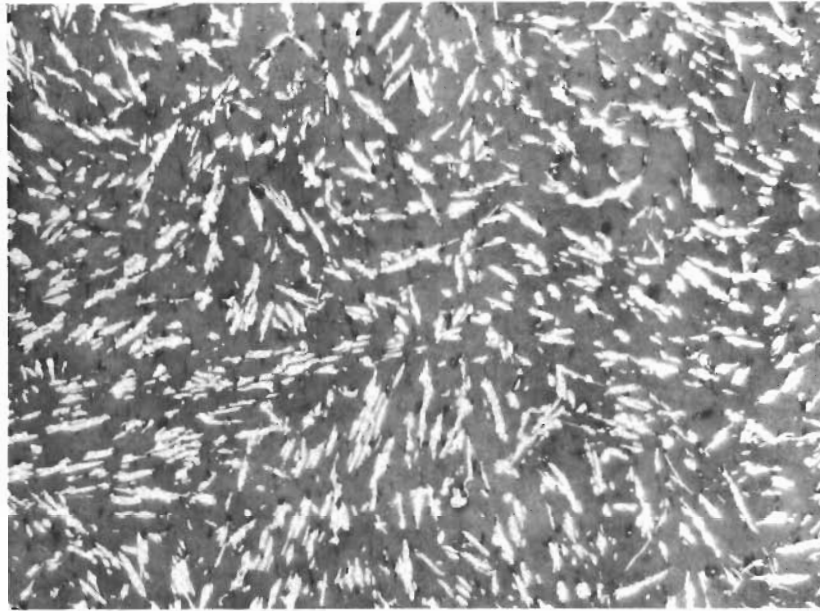


Figure 9. Hf-B (13 At% B), Rapidly Quenched from 1900°C. X500
Hf + HfB Eutectic.

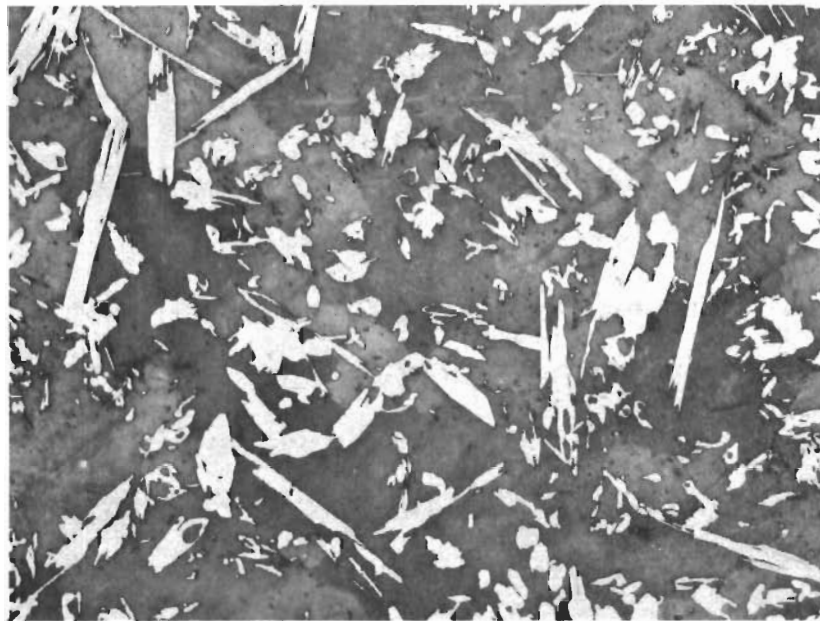


Figure 10. Hf-B (20 At% B), Quenched with $\sim 8^\circ\text{C}$ per
Second from 1900°C. X600
Primary Monoboride in a Matrix of Largely Segregated
Hf + HfB Eutectic.



Figure 11. Hf-B (30 At% B), Quenched with Approximately 20°C per Second from 1910°C. X500

Primary Monoboride, and Hf + HfB Eutectic (Partially Segregated).

X-ray: α -Hf + HfB

diboride was noticed in the alloy with 48 atomic percent, which was quenched from slightly above the peritectic line; no monoboride was present in the alloys quenched from temperatures far above the peritectic line (Table 3). The very sluggish back-reaction, usually superimposed onto the solidification peak of the rest eutectic was also noticed in the DTA-experiments (Figures 12 and 13).

Metallographically, the peritectic reaction could be traced down to boron concentrations of less than 30 atomic percent and usually preceded to completion if the total boron content was less than 35 atomic percent and the cooling rates employed did not exceed 4°C per second (Figures 14 through 16).

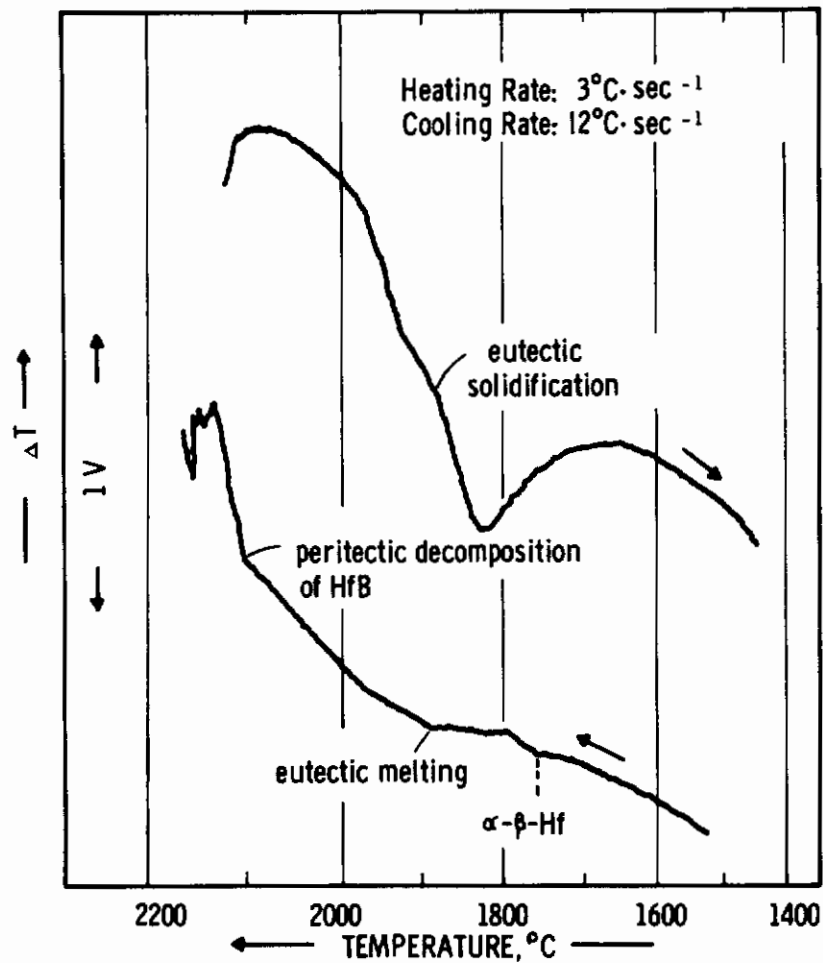


Figure 12. DTA-Thermogram of a Hafnium-Boron Alloy with 40 Atomic Percent Boron.

Note Bivariant Melting Between 1900 and 2100°C on the Heating, and Partial Superposition of Peritectic and Eutectic Reaction on the Cooling Cycle.

X-ray After the Run: $\text{Hf} + \text{HfB} + \text{HfB}_2$

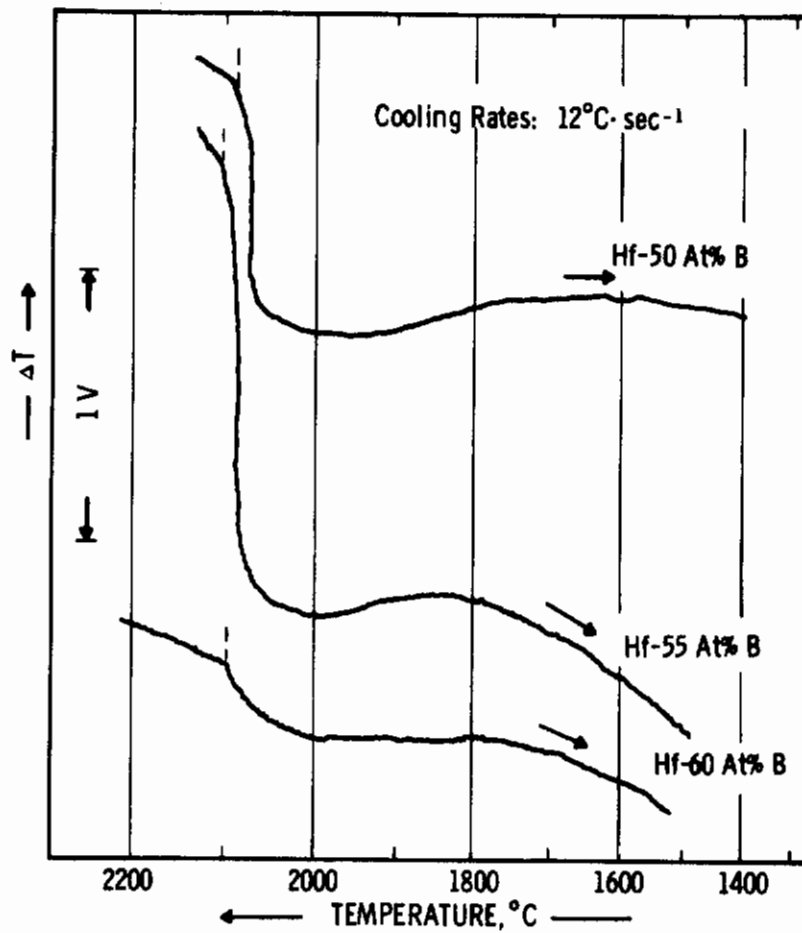


Figure 13. DTA-Thermograms (Cooling) of Hafnium-Boron Alloys from the Concentration Range 50 to 60 At% B.

Spreaded Peaks Indicate Superposition of Eutectic and Peritectic Reaction.

X-rays After the Runs: $\text{Hf} + \text{HfB}_2 +$ Smaller Quantities of Monoboride.

Contrails

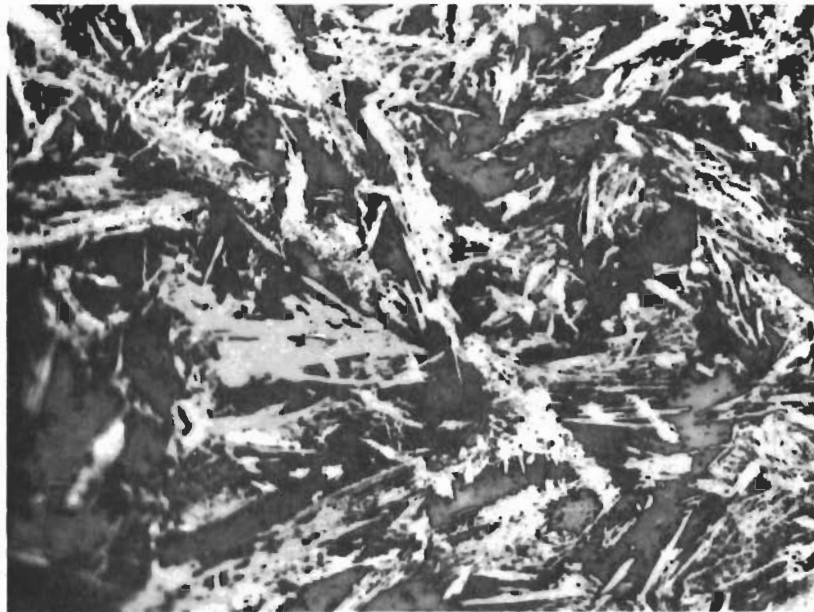


Figure 14. Hf-B (30 At% B), Cooled with 3°C per Second X1000
from 2130°C.

Hafnium (Dark) and HfB, Formed in a Peritectic Reaction
Between Melt and Diboride.

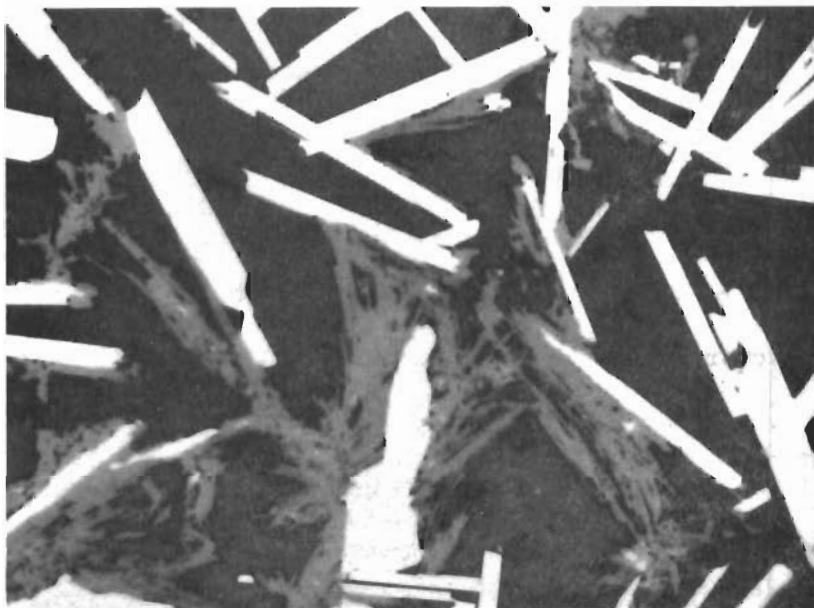


Figure 15. Hf-B (35 At% B), Cooled with 8°C per Second X1000
from 2150°C.

Initiation of Peritectic Reaction $P + \text{HfB}_2 \rightarrow \text{HfB}$.



Figure 16. Hf-B (30 At% B), Alloy from Figure 14
Annealed for 225 hrs at 1650°C.

X850

Hf (Light), and Dark-Colored HfB.

While in the alloys with compositions less than 40 atomic percent, the peritectic formation of the monoboride from diboride and melt appears fairly obvious from the appearance of the microstructures, chance nucleation within the metal phase, followed by continued growth of the monoboride nuclei in the direction of the boron-source (HfB_2), seems to be the predominant factor if the reaction in non-equilibrium mixtures $\text{Hf} + \text{HfB}_2$ is allowed to proceed at subsolidus temperatures (Figures 16 through 22). Nucleation of the monoboride phase, which appears to be the rate-controlling step, occurs fairly rapidly at temperatures close to liquidus, and the minimum amount of monoboride required for adequate growth propagation at lower temperatures can also be formed comparatively fast by direct attack of the melt on the diboride at temperatures between eutectic and peritectic

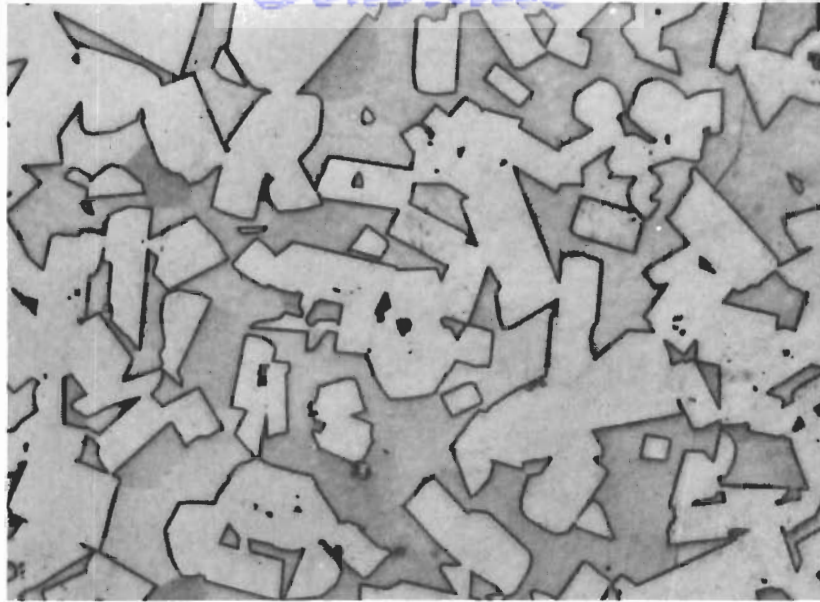


Figure 17. Hf-B (40 At% B), Reannealed for 225 hrs. at 1650°C X1000
After Rapid Quenching from 2500°C.
HfB₂ + Hf (Somewhat Darker Shaded)
X-ray: Hf + HfB₂

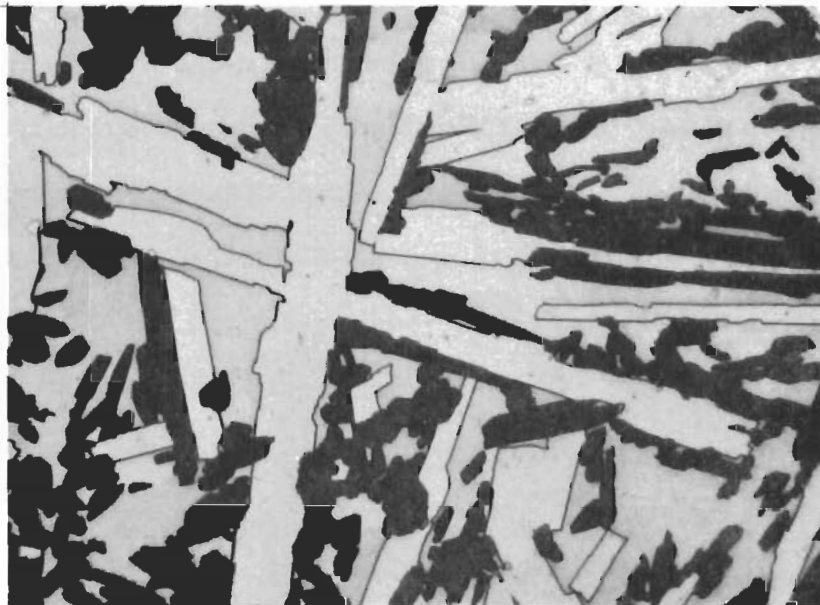


Figure 18. Hf-B (40 At% B), Quenched from 2500°C ; X750
Annealing: 1 Minute at 1850°C to 1880°C,
Followed by 225 hrs at 1650°C.
HfB₂ (Light, Acicular Shaped), Hafnium (Slightly Shaded),
and Hafnium Monoboride (Dark).
X-ray: Hf + HfB + HfB₂

line (Figures 19, 21, 22). However, practically no monoboride is formed upon reannealing of rapidly quenched ($> 2200^{\circ}\text{C}$) alloys at temperatures below 1650°C (Figure 17).

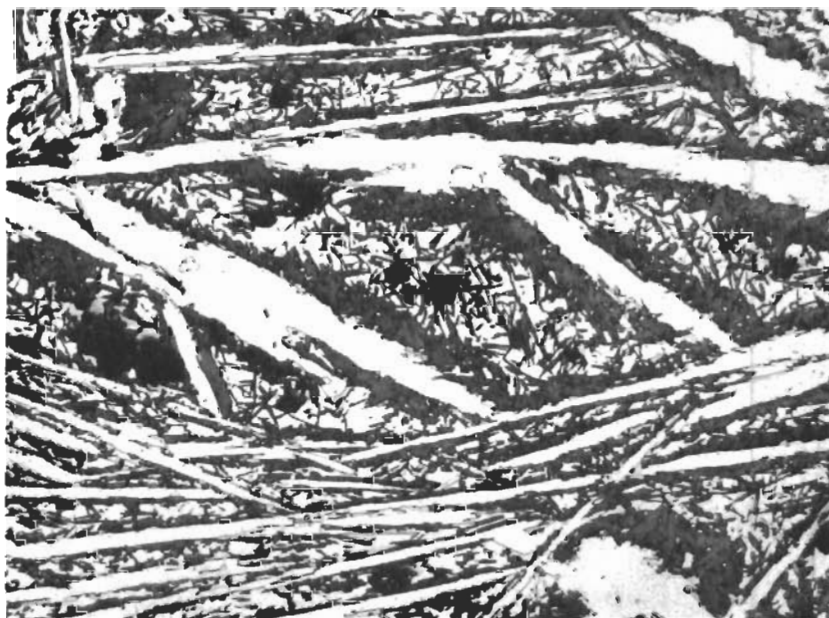


Figure 19. Hf-B (40 At% B), Quenched from 2500°C .
Annealing: 2 Minutes at $\sim 1950^{\circ}\text{C}$, Followed
by 225 hrs at 1650°C .

X120

$\text{Hf} + \text{HfB}_2 + \text{HfB}$ (Dark Phase)

Note Initial Peritectic Attack of Diboride by the Metal-Rich Melt, and the Random Distribution of Monoboride Within the Metal Grains.

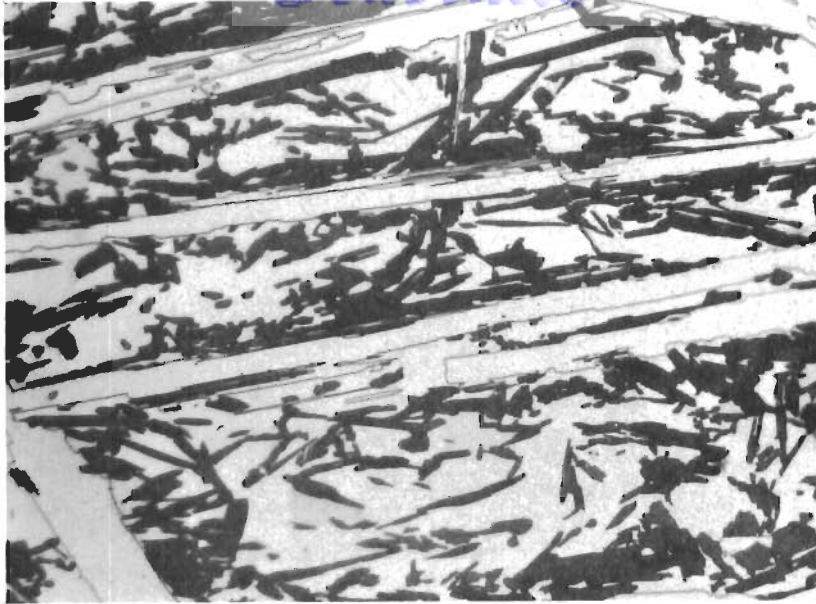


Figure 20 a.

X400

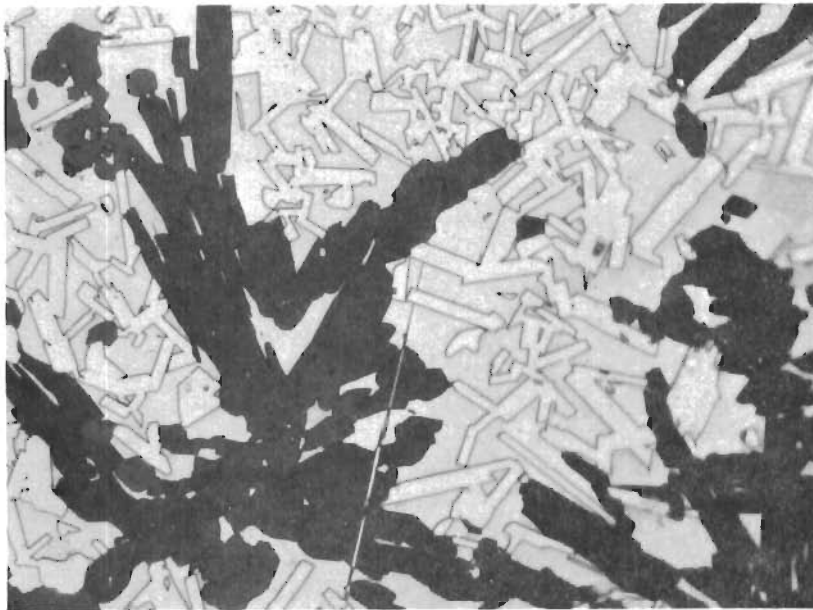


Figure 20 b.

X600

Figure 20 a) and b). Hf-B (46 At% B), Quenched from 2600°C, and Heat-Treated for 12 hrs at 1750°C.

Nucleation and Growth of Hafnium Monoboride in the Metal Matrix.

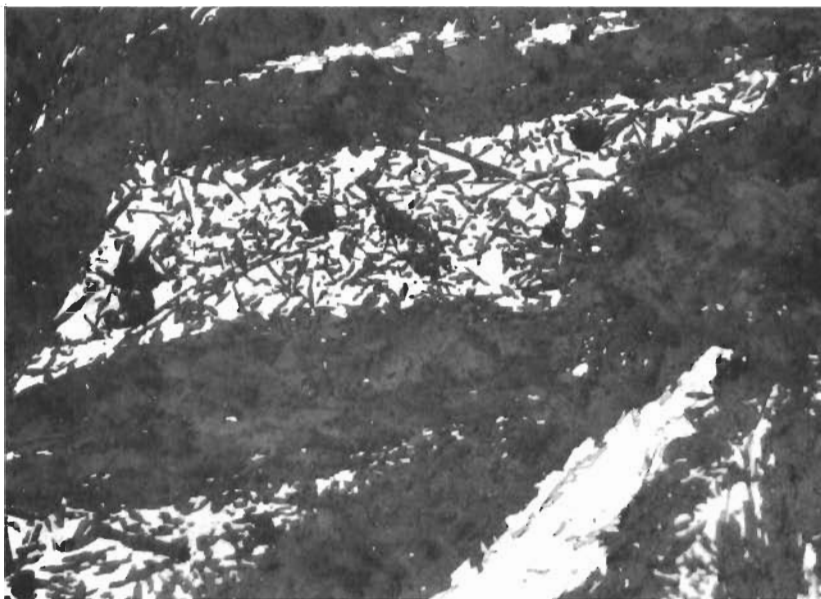


Figure 21. Hf-B (46 At% B), Quenched from 2500°C .
Annealing: 10 Minutes at 2050°C, Followed
by 225 hrs at 1650°C.

X250

Hf, HfB (Dark), and Rest Amounts of Hafnium Diboride
(Light Grains, Surrounded by Hafnium Monoboride).

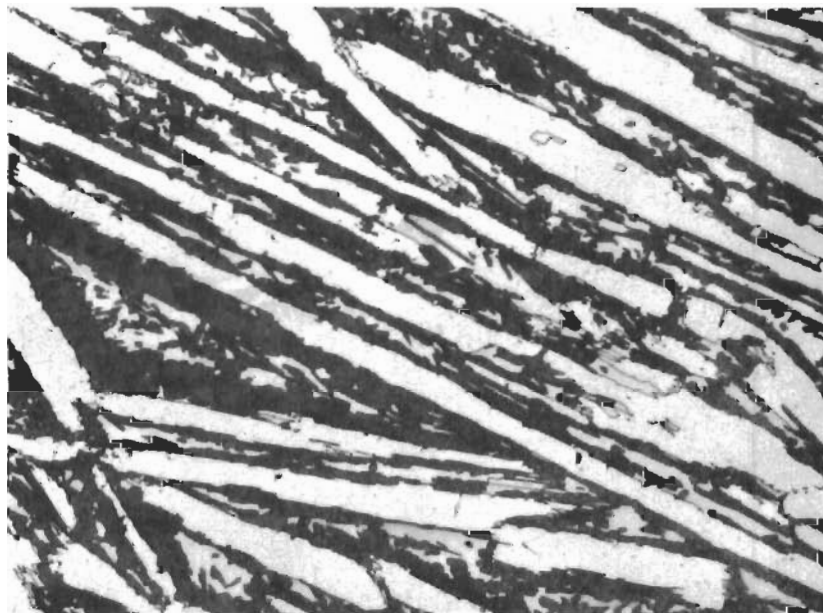


Figure 22 a. 6 Hours at 1750°C

X325

Contrails

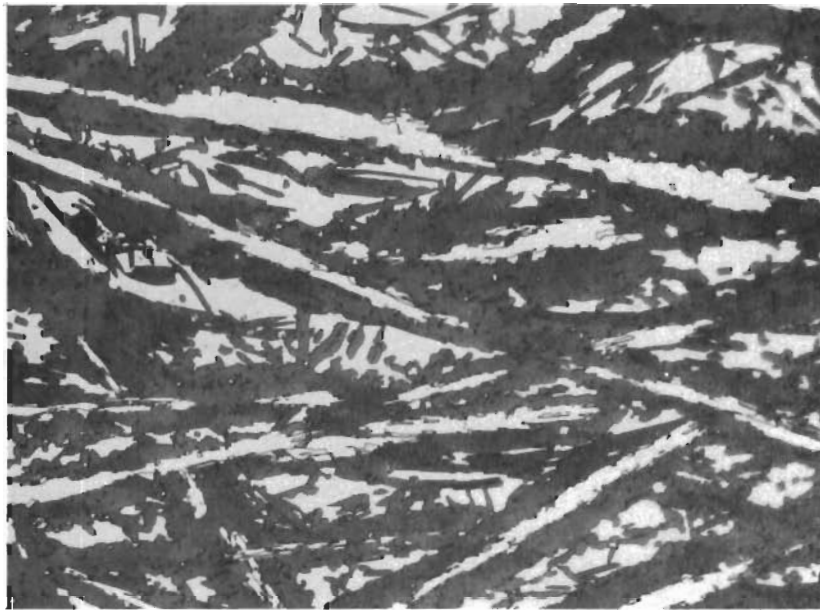


Figure 22 b

12 Hours at 1750°C

X375

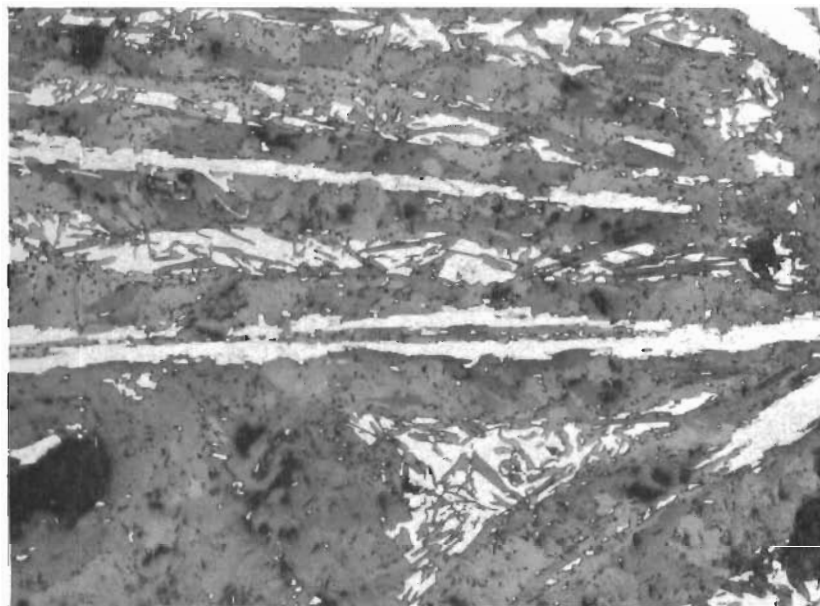


Figure 22 c

12 Hours at 1750°C + 225 Hours at 1650°C

X325

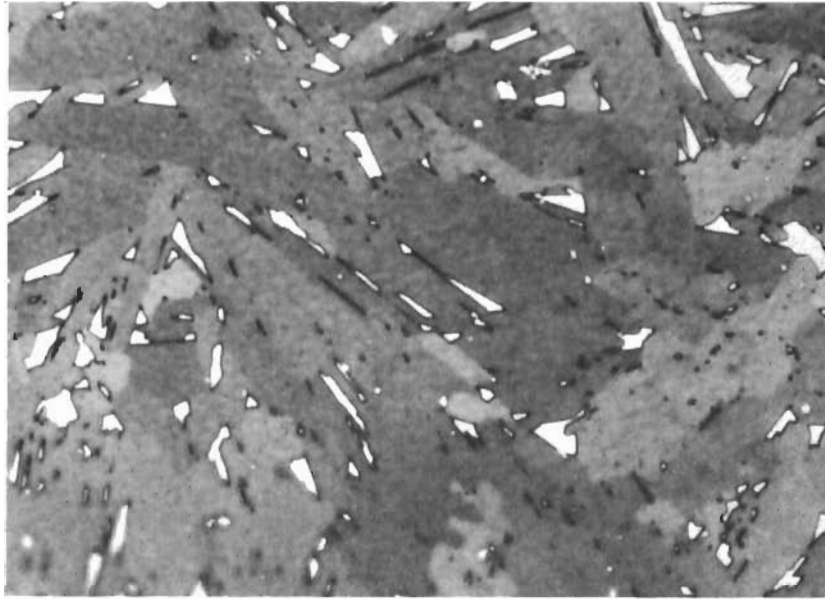


Figure 22 d. 225 Hours at 1650°C + 243 Hours at 1750°C. X1000
Hafnium Monoboride and Small Amounts of
Excess Hafnium (Light Grains).

Figures 22 a) through 22 d):

Hf-B (48 At% B), Quenched from 2600°C. Nucleation of the
Monoboride: 2 Minutes at 2050°C.

Formation of Hafnium Monoboride from Diboride and Hafnium
After Prolonged Heat Treatments at Subsolidus Temperatures.

Contrails

Although inconclusive, it seems to be worthwhile to mention, that the experimental observations also indicate a certain dependence of the rate of back-reaction upon the degree of superheating ($T_{\text{equil.}} - T_{\text{peritect.}}$) of the alloys prior to quenching. One may suspect, that this phenomenon will have to do with temperature changes of a monoboride-type short range order prevailing in the melt at lower temperatures. Related effects have frequently been observed in solid state decompositions of inorganic salts, such as carbonates, etc. ("Erinnerungsvermögen").

X-ray inspection of monoboride-containing alloys, which were reannealed for 160 hours at 1250° showed a slight, but noticeable decrease of the amount of monoboride. This observation is in accordance with our previous findings^(6, 7), which indicated that HfB might undergo a decomposition towards lower temperature. However, prolonged heat treatment studies (> 1000 hrs) at these temperatures will be necessary in order to obtain a definitive answer to this problem.

Lattice parameter measurements on solid state equilibrated samples showed practically no change of the cell dimensions of hafnium monoboride with the boron concentration; thus, the homogeneity range of the phase must be very small, probably less than one atomic percent. The average parameters measured were $a = 6.517 \text{ \AA}$, $b = 3.218 \text{ \AA}$, $c = 4.920 \text{ \AA}$, which are in good agreement with the parameters derived in the initial structure determination^(6, 7) (Table 2). Micrographic inspection of the alloys further indicated [compare for example Figure 22 (d)] that the phase is located at compositions close to stoichiometry.

3. Hafnium Diboride, and Boron-Rich Equilibria

Alloys from the concentration range 60 to 33 atomic percent boron melted extremely two-phased; due to the small amounts of

melt formed in these alloys, incipient melting generally could not be observed until temperatures were reached, which were appreciably above the peritectic line. Maximum melting, substantiated by a total of 16 measurements in this concentration range, occurs at 3380° and at a composition of ~66 atomic percent boron. Two-phased melting again was noted in specimens with analyzed boron contents of 67.4 and 68.6 atomic percent.

The small homogeneity range of the diboride was independently verified by lattice parameter calculations on an alloy series which was equilibrated and then rapidly quenched from 2000°C (Figure 23): Within the experimental error limits, no variation of the lattice dimensions with the boron concentration could be detected and no signs of precipitations, which could be related to temperature-dependent phase boundaries, could be found metallographically. As a matter of fact, due to the narrow homogeneous range of the phase, it proved to be quite difficult to prepare truly single-phased material (Figures 24 through 26).

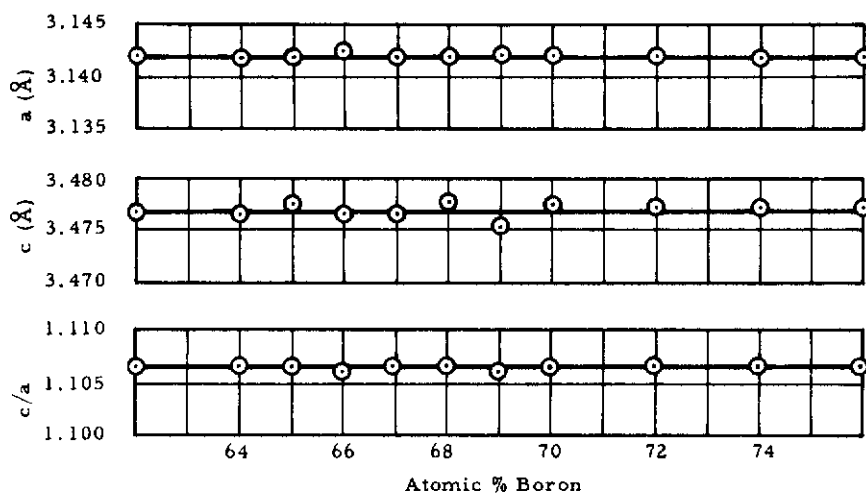


Figure 23. Lattice Parameters of Hafnium Diboride as a Function of the Boron Content.

(Alloys Rapidly Quenched from 2000°C)

Contrails

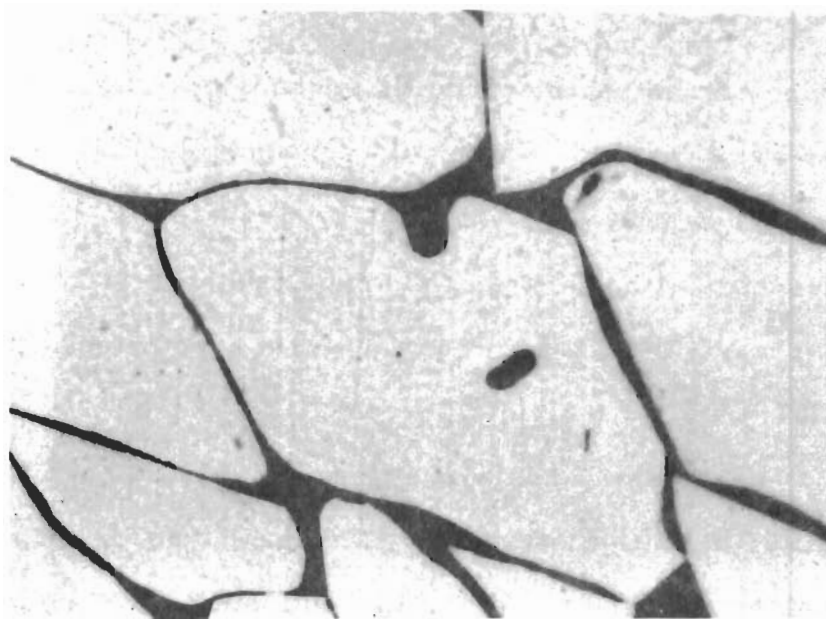


Figure 24. Hf-B (63.0 At% B), Rapidly Cooled from 2600°C. X1000
Hafnium Diboride and Excess Hafnium (Dark).

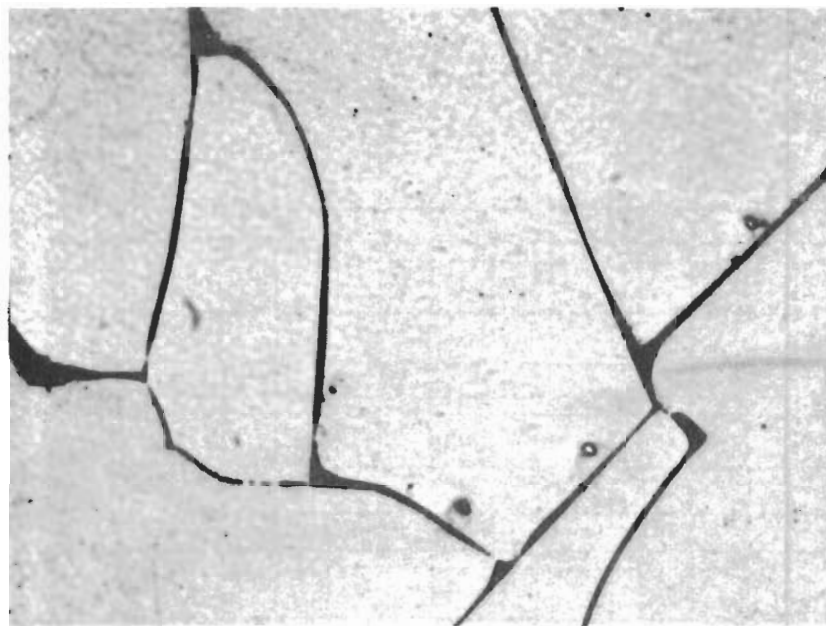


Figure 25. Hf-B (64.8 At% B), Rapidly Cooled from 2700°C. X1000
Hafnium Diboride and Small Amounts of Grain Boundary
Hafnium.

Contrails

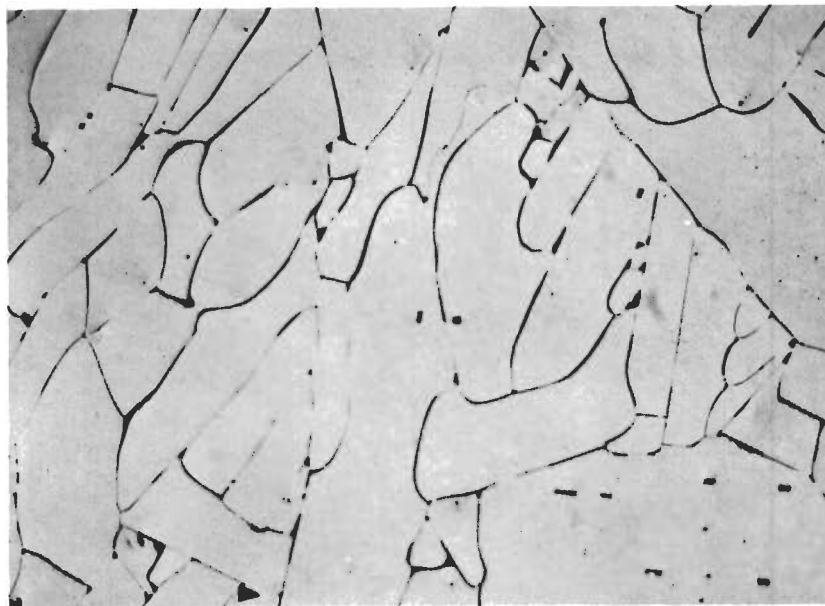


Figure 26 a. 65.3 ± 0.3 At%, 2800°C
 $\text{HfB}_2 + \text{Hf}$

X250

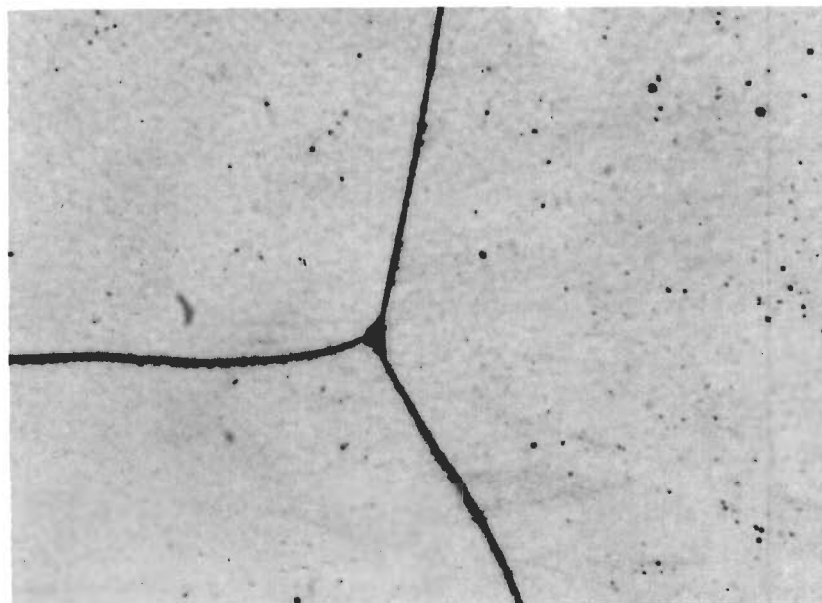


Figure 26 b. 65.6 ± 0.3 At%, 2800°C
 $\text{HfB}_2 + \text{Hf}$

X1000

Contrails

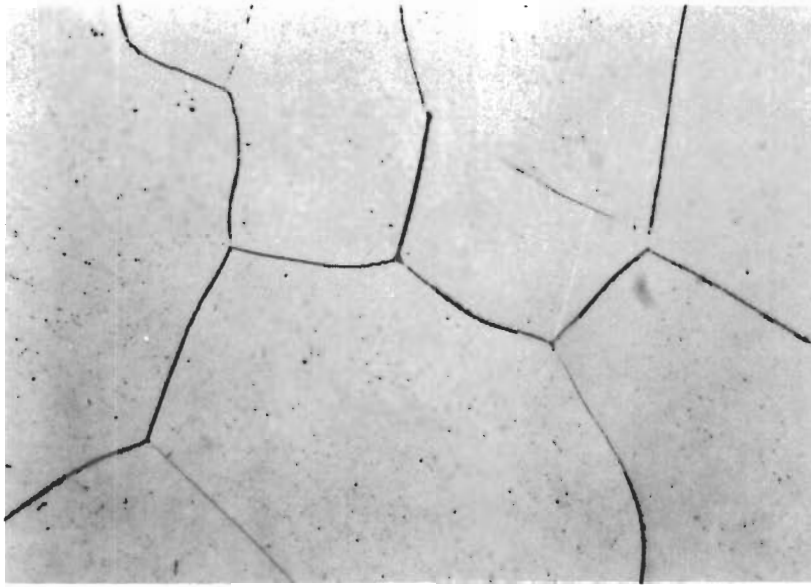


Figure 26 c. 66.0 ± 0.3 At%, 2800°C
HfB₂ + Trace Hf

X400

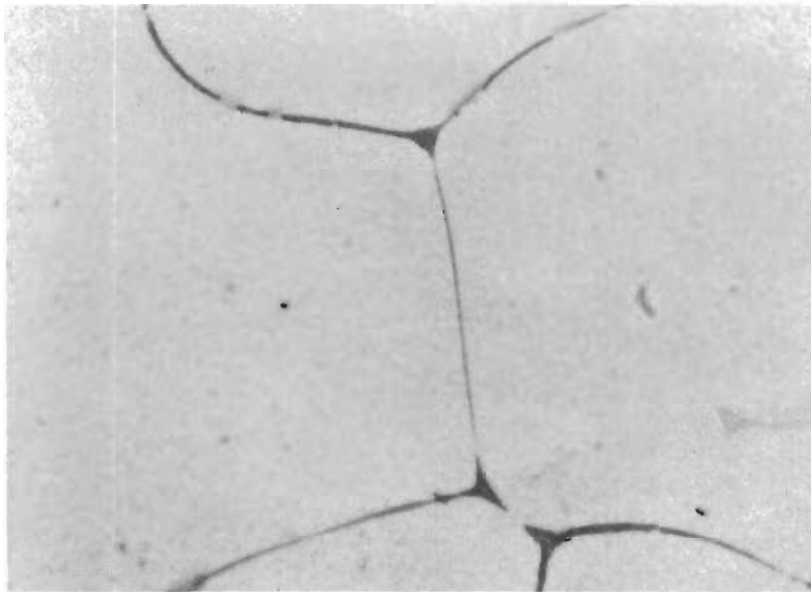


Figure 26 d. 66.6 ± 0.3 At% B, 2400°C
HfB₂ + Trace Boron

X1000

Contrails

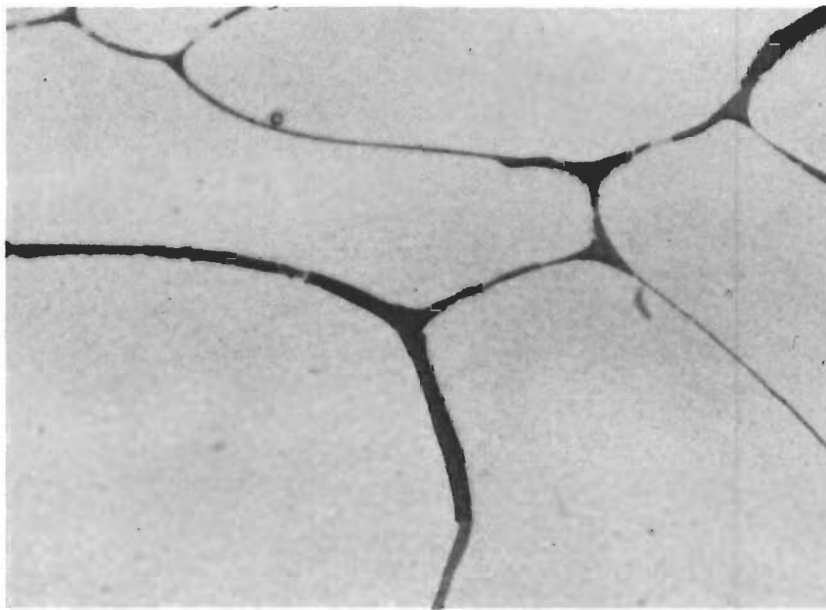


Figure 26 e. 67.0 ± 0.3 At%, 2400°C
HfB₂ + Trace Boron

X900

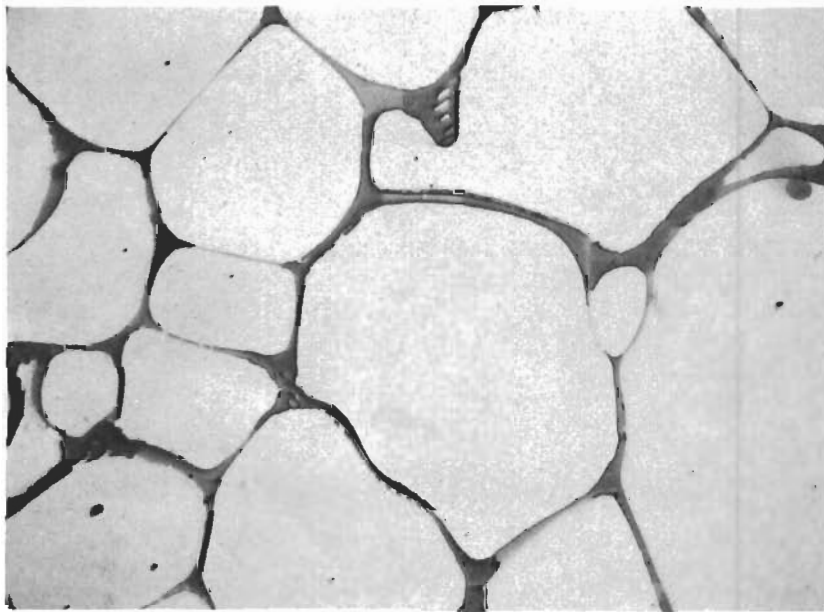


Figure 26 f. 67.5 ± 0.3 At%, 2800°C
HfB₂ + B

X450

Contrails

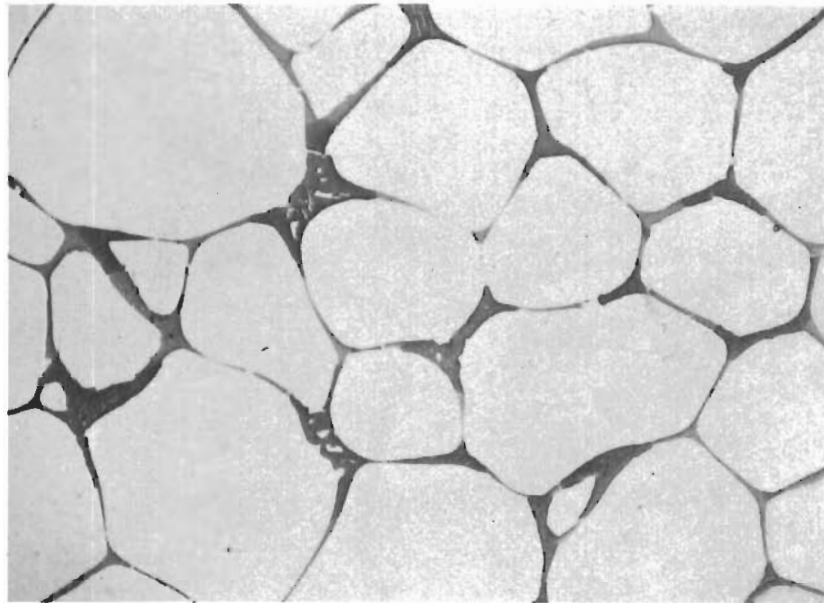


Figure 26 g. 67.9 ± 0.3 At% B, 2900°C

X500

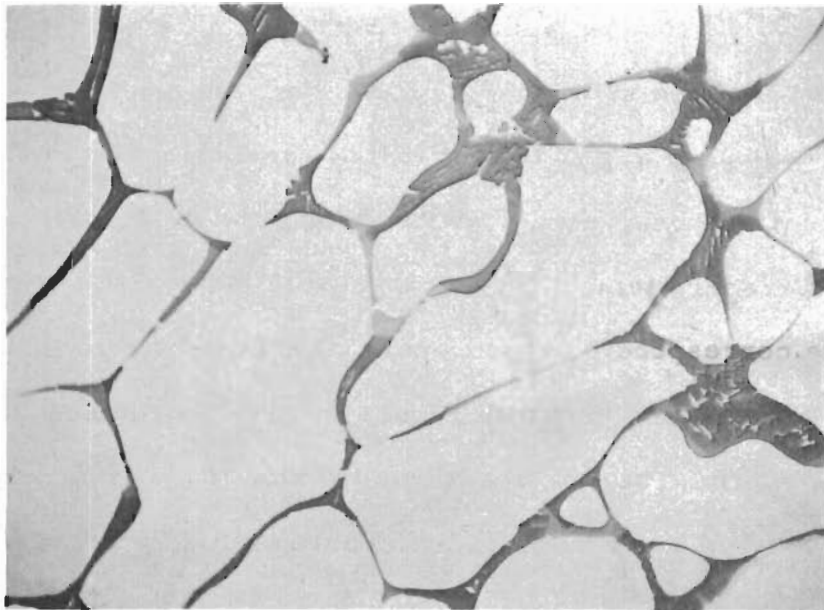
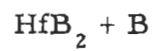
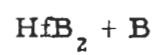


Figure 26 h. 68.8 ± 0.5 At% B, 2800°C

X400



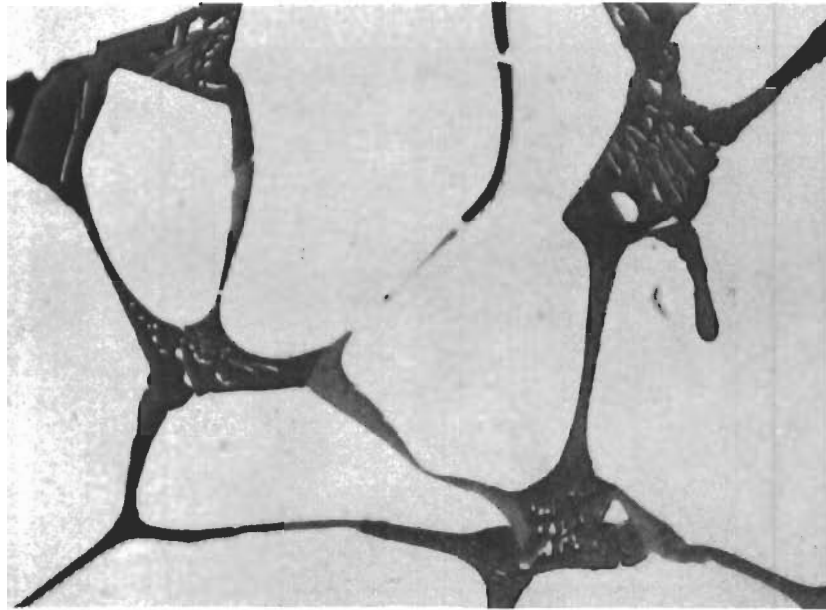
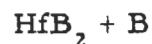


Figure 26 i. 72 At% B, 2800°C.

X750



Melting point determinations on high-boron (> 85 At% B) were difficult to perform with the Pirani-method; the electrical conductivity of the samples was poor at low temperatures, and preheating of the samples with a foreign heat source, such as described in the experimental work on the zirconium-boron system⁽¹²⁾, did not provide the desired accuracy (Table 3). The corresponding experimental points were therefore omitted in the compilation drawing shown in Figure 2. The finally accepted temperature for the boron-rich eutectic reaction isotherm (Figure 1) is based mainly upon results gained in the differential-thermoanalytical studies (Figure 27).

Metallographic examination of arc melted specimens with boron concentrations between 90 and 99 atomic percent always showed primary crystallized hafnium diboride in a eutectic matrix, which contained

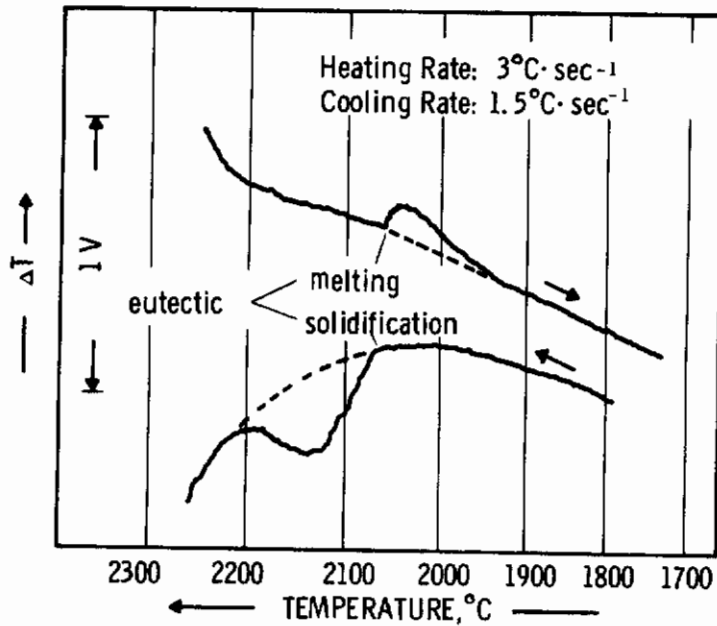


Figure 27. DTA-Thermogram of a Hafnium-Boron Alloy with 80 Atomic Percent Boron.

only minute quantities of diboride. The higher diboride contents of the eutectic, as suggested by the microstructures shown in Figure 26 (a) through 26 (i), apparently must have been caused by trapping of diboride crystals in the boron-rich melt during the rapid quenching process. Generally, the microstructures of the high-boron alloys were of comparable poor quality and were therefore not taken up in the report.

IV. DISCUSSION

A comparison of the three group IV metal-boron systems reveals, that zirconium-boron falls somewhat out of line in its phase behavior, as no stable monoboride is formed; on the other hand, a dodecaboride only exists in the zirconium-boron system, whereas no phases richer in boron than the diboride occur in the other two group IV metal-boron systems. Although no detailed thermodynamic quantities are available for either compounds other than the diborides, a somewhat closer inspection of the phase diagrams indicates only marginal relative stabilities for TiB and HfB , as well as for the dodecaboride in the zirconium-boron system. Thus, one may suspect, that only small variations in the stabilities of the diborides would be necessary to control the appearances of phases other than the diborides in these systems; an immediate decision, whether, say, the hypothetical zirconium monoboride is of lower stability than its counterparts in the titanium- and hafnium-boron systems, may therefore be deceiving. Quantitative comparisons for cases where instable compounds are involved, are only possible from an thermodynamic evaluation of the equilibria in higher order systems⁽¹⁶⁾. For the specific boride phases under discussion, such a comparative analysis is presently being performed using data from ternary phase equilibria in the systems $Ti-Hf-B$, $Ti-Zr-B$, and $Zr-Hf-B$, and the results will be summarized in another report issued under the present program.

REFERENCES

- 1 L. Kaufman and E.V. Clougherty: RTD-TDR-63-4096, Part II (Feb. 1965).
- 2 F.W. Glaser, D. Moskowitz, and B.W. Post: J. Metals, 5 (1953), 1119.
- 3 K. Moers: Z. anorg. allg. Chem. 198 (1931), 262.
- 4 C. Agte and K. Moers: Z. anorg. allg. Chem. 198 (1931), 233.
- 5 R. Kieffer, F. Benesovsky, and E.R. Honak: Z. anorg. allg. Chemie, 268 (1952), 191.
- 6 E. Rudy and F. Benesovsky: Mh.Chem. 92 (1961), 415.
- 7 E. Rudy: Thesis, Technische Hochschule Wien (1960).
- 8 H. Nowotny, H. Braun, and F. Benesovsky: Radex Rundphan 6 (1960), 367.
- 9 R. Kieffer and F. Benesovsky: Hartstoffe (Wien, Springer, 1963).
- 10 W.B. Pearson: Handbook of Lattice Spacings and Structures of Metals and Alloys (Pergamon Press, New York, 1958).
- 11 E. Rudy: AFML-TR-65-2, Part I, Vol. IV (Sept. 1965).
- 12 E. Rudy and St. Windisch: AFML-TR-65-2, Part I, Vol. VIII (Oct 1965).
- 13 E. Rudy, St. Windisch, and Y.A. Chang: AFML-TR-65-2, Part I, Vol. I (Jan 1965).
- 14 E. Rudy and St. Windisch: AFML-TR-65-2, Part I, Vol. VII (Oct. 1965).
- 15 H. Heetderks, E. Rudy, and T. Eckert: AFML-TR-65-2, Part III, Vol. I, May 1965 (Planseeber. Pulvermet. 13, 1965, page 105).
- 16 E. Rudy: Z. Metallkde, 54 (1963), 112.

Unclassified
Security Classification

DOCUMENT CONTROL DATA - R&D		
<i>(Security classification of title, body of abstract and indexing annotation must be entered when the overall report is classified)</i>		
1. ORIGINATING ACTIVITY (Corporate author) Materials Research Laboratory Aerojet-General Corporation Sacramento, California		2a. REPORT SECURITY CLASSIFICATION Unclassified
		2b. GROUP N/A
3. REPORT TITLE Ternary Phase Equilibria in Transition Metal-Boron-Carbon-Silicon Systems Part I. Related Binary Systems. Volume IX. Hf-B System		
4. DESCRIPTIVE NOTES (Type of report and inclusive dates)		
5. AUTHOR(S) (Last name, first name, initial) E. Rudy St. Windisch		
6. REPORT DATE January 1966	7a. TOTAL NO. OF PAGES 42	7b. NO. OF REFS 16
8a. CONTRACT OR GRANT NO. AF33(615)-1249	9a. ORIGINATOR'S REPORT NUMBER(S) AFML TR 65-2 Part I. Vol. IX	
b. PROJECT NO. 7350 735001	9b. OTHER REPORT NO(S) (Any other numbers that may be assigned this report) N/A	
c.		
d.		
10. AVAILABILITY/LIMITATION NOTICES This document is subject to special export controls and each transmittal to foreign governments or foreign nationals may be made only with prior approval of the Air Force Materials Laboratory (MAM), Wright- Patterson Air Force Base, Ohio.		
11. SUPPLEMENTARY NOTES	12. SPONSORING MILITARY ACTIVITY AFML(MAMC) Wright-Patterson AFB, Ohio 45433	
13. ABSTRACT The binary alloy system hafnium-boron has been investigated by means of X-ray, metallographic, melting point, and differential-thermoanalytical techniques. The experimental alloy material comprised of hot-pressed and heat-treated, arc- and electron-beam melted, as well as equilibrated and quenched alloy material. All phases of the experimental investigations were supported by chemical analysis. The results of the present investigation, which resulted in the establishment of a complete phase diagram for the system, are discussed and compared with previously established system data.		

14.	KEY WORDS	LINK A		LINK B		LINK C	
		ROLE	WT	ROLE	WT	ROLE	WT
	Binary Hafnium-Boron High Temperature Phase Equilibria						

INSTRUCTIONS

1. ORIGINATING ACTIVITY: Enter the name and address of the contractor, subcontractor, grantee, Department of Defense activity or other organization (*corporate author*) issuing the report.

2a. REPORT SECURITY CLASSIFICATION: Enter the overall security classification of the report. Indicate whether "Restricted Data" is included. Marking is to be in accordance with appropriate security regulations.

2b. GROUP: Automatic downgrading is specified in DoD Directive 5200.10 and Armed Forces Industrial Manual. Enter the group number. Also, when applicable, show that optional markings have been used for Group 3 and Group 4 as authorized.

3. REPORT TITLE: Enter the complete report title in all capital letters. Titles in all cases should be unclassified. If a meaningful title cannot be selected without classification, show title classification in all capitals in parenthesis immediately following the title.

4. DESCRIPTIVE NOTES: If appropriate, enter the type of report, e.g., interim, progress, summary, annual, or final. Give the inclusive dates when a specific reporting period is covered.

5. AUTHOR(S): Enter the name(s) of author(s) as shown on or in the report. Enter last name, first name, middle initial. If military, show rank and branch of service. The name of the principal author is an absolute minimum requirement.

6. REPORT DATE: Enter the date of the report as day, month, year, or month, year. If more than one date appears on the report, use date of publication.

7a. TOTAL NUMBER OF PAGES: The total page count should follow normal pagination procedures, i.e., enter the number of pages containing information.

7b. NUMBER OF REFERENCES: Enter the total number of references cited in the report.

8a. CONTRACT OR GRANT NUMBER: If appropriate, enter the applicable number of the contract or grant under which the report was written.

8b, 8c, & 8d. PROJECT NUMBER: Enter the appropriate military department identification, such as project number, subproject number, system numbers, task number, etc.

9a. ORIGINATOR'S REPORT NUMBER(S): Enter the official report number by which the document will be identified and controlled by the originating activity. This number must be unique to this report.

9b. OTHER REPORT NUMBER(S): If the report has been assigned any other report numbers (*either by the originator or by the sponsor*), also enter this number(s).

10. AVAILABILITY/LIMITATION NOTICES: Enter any limitations on further dissemination of the report, other than those

imposed by security classification, using standard statements such as:

- (1) "Qualified requesters may obtain copies of this report from DDC."
- (2) "Foreign announcement and dissemination of this report by DDC is not authorized."
- (3) "U. S. Government agencies may obtain copies of this report directly from DDC. Other qualified DDC users shall request through _____."
- (4) "U. S. military agencies may obtain copies of this report directly from DDC. Other qualified users shall request through _____."
- (5) "All distribution of this report is controlled. Qualified DDC users shall request through _____."

If the report has been furnished to the Office of Technical Services, Department of Commerce, for sale to the public, indicate this fact and enter the price, if known.

11. SUPPLEMENTARY NOTES: Use for additional explanatory notes.

12. SPONSORING MILITARY ACTIVITY: Enter the name of the departmental project office or laboratory sponsoring (*paying for*) the research and development. Include address.

13. ABSTRACT: Enter an abstract giving a brief and factual summary of the document indicative of the report, even though it may also appear elsewhere in the body of the technical report. If additional space is required, a continuation sheet shall be attached.

It is highly desirable that the abstract of classified reports be unclassified. Each paragraph of the abstract shall end with an indication of the military security classification of the information in the paragraph, represented as (TS), (S), (C), or (U).

There is no limitation on the length of the abstract. However, the suggested length is from 150 to 225 words.

14. KEY WORDS: Key words are technically meaningful terms or short phrases that characterize a report and may be used as index entries for cataloging the report. Key words must be selected so that no security classification is required. Identifiers, such as equipment model designation, trade name, military project code name, geographic location, may be used as key words but will be followed by an indication of technical context. The assignment of links, rules, and weights is optional.